Alpine Proglacial Stream Temperature Dynamics

by

John Richards

B.A. (Hons), University of Oxford, 2006

A THESIS SUBMITTED IN PARTIAL FULFILMENT OF
THE REQUIREMENTS FOR THE DEGREE OF

Master of Science

in

The Faculty of Graduate Studies

(Geography)

The University of British Columbia

(Vancouver)

August, 2008

Abstract

This study was motivated by an interest in understanding the effects of glacier retreat on late summer stream temperatures in an above-treeline proglacial stream and lake system in the southern Coast Mountains of British Columbia, Canada. Fieldwork was carried out during August and September of 2007 and focused on thermal processes controlling water temperature in the proglacial lake and a 1 km alpine reach directly downstream of the lake outlet. The proglacial lake was small (0.07 km^2), featured a single inflow and outflow channel and had a residence time of approximately 4 days. The alpine reach featured continual cascading flow (25% channel gradient), marked diurnal fluctuations in discharge and variable terrain shading.

It was found that warming between the inflow and outflow of the lake (1.8 °C, on average) was controlled by the total heat content of the lake and cycles of mixing and stratification. A heat budget analysis indicated that the heat content of the lake was dominantly controlled by absorbed shortwave radiation and the advective effect of the inflow and outflow streams. Application of a dynamic reservoir model (DYRESM) to model observed lake temperatures (inflow, outflow and a temperature-depth profile), and comparison to other studies, suggested that suspended sediment concentration in the inflow had a dominant control on lake mixing and stratification.

Based on equations developed from low-gradient channels, a stream energy budget model failed to replicate observed downstream warming rates. A spatially distributed net radiation model, along with statistical modification of the energy budget, provided insight into the pro-

cesses that control stream temperatures in alpine areas. The final hybrid model showed a good match with observed downstream warming. This model accounted for the variation of width and albedo with discharge, and the spatial variability in net radiation due to topographic shading and the slope and aspect of the channel. The model also included parameters that increased the sensible and latent heat fluxes relative to values calculated from standard equations, which is consistent with the hypothesis that these fluxes are enhanced by cascading flow.

Table of Contents

Abstract ii

Table of Contents iv

List of Tables vii

List of Figures viii

Acknowledgements xi

1 Introduction 1

1.1 Motivation for the study 1

1.2 Literature review 3

1.2.1 Physical controls on stream temperature 3

1.2.2 Thermal effect of a proglacial lake 5

1.3 Research objectives 7

1.4 Thesis outline 8

2 Study area and methods 9

2.1 Study Area 9

2.2 Data collection and processing 13

2.2.1 Water temperature measurement 13

2.2.2 Meteorological data 14
2.2.3 Discharge measurement 16
2.2.4 Calculation of lake inflow 20
2.3 Calculation of surface heat fluxes 20
2.3.1 Solar radiation 21
2.3.2 Longwave radiation 24
2.3.3 Latent and sensible heat fluxes 24
2.4 Calculation of lake heat budget 25
2.5 Lake modelling 26
2.5.1 CSTR model 26
2.5.2 Epilimnion model 28
2.5.3 DYRESM 28
2.6 Stream heat budget modelling 31
2.6.1 Description of models 31
2.6.2 Calculation of goodness-of-fit statistics 32

3 Results 34
3.1 Overview of study period 34
3.2 Place Lake 37
3.2.1 Observed temperature trends 37
3.2.2 Radiation modelling at Place Lake 39
3.2.3 Lake heat budget 40
3.2.4 Lake modelling 43
3.3 Alpine Reach 47
3.3.1 Overview 47
3.3.2 Radiation model performance 47

3.3.3 Stream heat budget modelling results 50

4 Discussion 57

4.1 Place Lake 57

4.1.1 Effect on stream temperature 57

4.1.2 Lake heat budget 59

4.1.3 Lake temperature modelling and controls on lake stability 59

4.1.4 Physical controls on outflow temperatures 62

4.2 Alpine reach 63

4.2.1 Modelling net radiation in an alpine stream 63

4.2.2 Alpine stream heat budget modelling 64

4.2.3 Warming rates 66

4.3 Implications for glacier retreat 68

4.3.1 Shifts in lake stability 68

4.3.2 Altered proglacial stream temperatures 69

5 Conclusions 71

5.1 Summary of key findings 71

5.1.1 Place Lake 71

5.1.2 Alpine reach 72

5.2 Future research 73

References 76

List of Tables

2.1 Instrument specifications 14

2.2 Sampling design 16

2.3 DYRESM input parameters 29

2.4 Summary of alpine energy budget models. Note that all four models are driven by reach averaged air and stream temperatures, reach averaged modelled net radiation, and discharge as measured at the lake outlet 32

3.1 Total energy added to Place Lake by each heat flux over the 23 day period . . . 42

3.2 Results of NLS analysis for two variants of Models 2 and 3 showing parameter estimates (p-value shown in parentheses), RMSE, MAE, MBE, AIC and I^2 (pseudo R^2) 52

4.1 Comparison of alpine lake studies 58

4.2 Comparison of alpine stream temperature studies 67

List of Figures

2.1 Map showing location of study area (adapted from map provided by R.D. Moore). 10

2.2 Map of study area (adapted from map provided by R.D. Moore). 11

2.3 Place Lake and Place Lake Meteorological Station. Inflow is at centre back and outflow in foreground. 12

2.4 Place Creek and Place Creek Meteorological Station. 12

2.5 Long profile of Place Creek from Place Lake outlet to the treeline 13

2.6 Aerial photograph of study area with highlighted stream channel and lake perimeters. Sampling sites are shown as black circles (photo courtesy of Eric Schiefer) . 15

2.7 Place Creek stage-discharge rating curve. Error bars indicate ±10% of the calculated discharge. 19

2.8 DYRESM simulation process in which 7 input files are required to produce the simulation file, which is then modified by the model program to produce an output simulation file which can be compared to observed data 30

3.1 Snowpack water equivalent at the Tenquille Lake snow course, including observed values for 2006 and 2007, as well as the minimum, maximum and mean values for the period of record (Source: B.C. Ministry of Environment Historical Snow Survey Data) 34

3.2 Vancouver International Airport long-term average (1971-2000) and 2007 mean monthly air temperatures 35
3.3 Time-series of (a) incident shortwave radiation at PM3, (b) stream temperature, (c) air temperature and (d) discharge at the lake outlet 36
3.4 Place Lake inflow, outflow and mid lake surface temperatures between August 24th and September 16th 37
3.5 Hydrometeorological conditions at Place Lake (a) Shows mid-lake temperatures at selected depths. (b), (c) and (d) show wind speed, air temperature and discharge at the lake outlet, respectively 38
3.6 Times series of observed (at PM3 and Ridge) and modelled averaged (a) incident shortwave radiation and (b) incident longwave radiation at Place Lake 40
3.7 Place lake heat fluxes in Wm^{-2}, where (a) is modelled averaged net shortwave radiation, (b) is modelled averaged incident longwave radiation, (c) is emitted longwave radiation, (d) is sensible heat flux, (e) is latent heat flux, (f) is energy associated with the inflow and outflow, and (g) is the total heat flux of Place Lake. (h) shows the heat content of the lake in MJm^{-2} 41
3.8 Place Lake outflow temperatures, modelled as a CSTR 44
3.9 Place Lake outflow temperatures, epilimnion model 44
3.10 Modelled and observed temperature profiles at Place Lake: (a) predicted by DYRESM run 1, (b) predicted by DYRESM run 2 and (c) observed. Note that the modelled surface fluctuates as a function of lake level, but the observed surface does not. 45
3.11 Time-series of observed and DYRESM modelled Place Lake temperatures at 6 depths from the surface 46
3.12 Observed stream warming between Place Creek MS and the treeline 47

3.13 Time series of water surface albedo values used in radiation model, parameterised as a power function of discharge 48
3.14 Scatter plots of predicted vs. observed net radiation for (a) observed versus modelled data at PCMS, and (b) observed versus reach averaged modelled data . 48
3.15 Time series of predicted and observed net radiation at PCMS for (a) a selected clear day, (b) a partially cloudy day and (c) an overcast day. (d), (e) and (f) show scatter plots of observed vs. modelled net radiation at the same site for selected days with similar cloud conditions to (a), (b) and (c), respectively 49
3.16 Observed versus predicted stream warming between Place Creek MS and the treeline for the four models, each with two variants. 51
3.17 Scatterplots of predictions from model 4b against observed downstream warming for (a) measured discharge, (b) half the measured discharge and (c) one-quarter the measured discharge 52
3.18 Measured and calculated heat fluxes in Wm^{-2} for the alpine reach: (a) net shortwave radiation, (b) incident longwave radiation, (c) emitted longwave radiation, (d) sensible heat flux, (e) latent heat flux, (f) modelled net radiation 54
3.19 Errors associated with Models 2b, 3b and 4b plotted over time and by hour . . . 55
3.20 (a) time series of observed and modelled stream warming for Model 3 using the reach averaged modelled net radiation, (b) associated errors for the same model 56

4.1 Inferred process responses to prolonged deglaciation from the hybrid heat budget modelling exercise 69

Acknowledgements

This research could not have been completed without the assistance of many people. I am grateful to my supervisor, Dan Moore, who assisted in generating ideas, provided guidance in the field and critical feedback throughout the analysis and write-up process. Marwan Hassan provided useful comments during the writing of this thesis.

I wish to thank Roger Hodson, Jason Leach, Joe Shea and Jon Clifton for their help in the field. Both Jason and Joe also made valuable contributions to the stream and lake radiation models. Joe provided two datasets from his own fieldwork on Place Glacier. Eric Schiefer provided aerial photographs. Alex Forrest and Megan Wolfe assisted in the calibration of DYRESM. The hard work of Ivan Liu played a key part in preparing for and designing the field set-up.

Funding for fieldwork was provided by Dan Moore via his Natural Sciences and Engineering Research Council Discovery Grant and by a grant from the Canadian Foundation for Climate and Atmospheric Sciences in support of the Western Canada Cryospheric Network. This project was completed while the author was recipient of a BUNAC Educational Trust Scholarship.

Chapter 1

Introduction

1.1 Motivation for the study

Stream temperature is an important water quality parameter for aquatic ecology. Most physical characteristics of water, as well as rates of biological and chemical reactions, are a function of stream temperature (Beschta et al., 1987). The integrity of an ecological system can be permanently altered by stream temperature changes as a result of land use and environmental change. Research has focused on physical controls, including insolation receipt, groundwater inflow, effects of storm events and local geomorphology (Malard et al., 2001; Malcolm et al., 2004), as well as the effects of forest harvesting, agriculture, urban development, and flow diversions (Brown, 1969; Klein, 1979; Hockey et al., 1982; Quinn et al., 1997; Gu et al., 1998; Moore et al., 2005b). Significant attention has also been devoted to the effects of climate change on stream temperatures (Mohseni et al., 2003; Morrill et al., 2005), but much of this work has been based on statistical relations between stream temperature and air temperature, with little regard for other physical controls (Moore, 2005b).

Recent work has also highlighted that glaciers play an important role in regulating summer stream temperatures in many parts of the world (Moore, 2006), and thus help to maintain optimal habitats for aquatic species such as salmonids (Fleming, 2005). Mountain glaciers have dominantly been retreating since the middle of the last century (IPCC, 2007) and it has been shown that this retreat is resulting in reduced late-summer streamflow in many parts of North

America (Moore, 2006; Stahl and Moore, 2006). Reduced streamflow could result in increased stream temperatures (Hockey et al., 1982; Gu et al., 1998; Webb et al., 2003), but there is still some uncertainty about the exact nature of this relationship, which has not been widely studied in alpine stream reaches.

Glacierised catchments possess a number of unique characteristics that influence stream temperature. Above-treeline reaches are particularly vulnerable to warming due to the intense insolation caused by the lack of shade and high elevation. Steep terrain results in variable stream shading, irregular channel morphology and cascading flow. The combination of snow melt, ice melt, groundwater and rain events results in dynamic source water contributions, which produce distinctive stream temperature dynamics (Brown et al., 2006). In a New Zealand glacierised catchment, Cadbury et al. (2008) found that the key drivers of the proglacial thermal regime were: (1) relative contribution from different water sources, (2) prevailing hydroclimatological conditions, (3) distance from source, (4) total stream flow volume and (5) basin geomorphology and riparian environment. High elevation proglacial lakes are another feature of the glacial environment that can act as a thermal regulator to through-flowing cold glacier melt water (Weirich, 1986; Uehlinger et al., 2003). Large sediment laden inflows contribute to mixing regimes that are uncommon to most other mid-latitude lakes and reservoirs (Wetzel, 1975; Weirich, 1986).

The overall objective of this study was to contribute to an understanding of the effects of glacier retreat on stream temperatures in an above-treeline reach of a proglacial stream and lake system. Achieving this objective required an examination of (1) the proglacial lake and (2) the proglacial stream channel. While the two parts of the study are largely treated separately due their individuality, the findings are very much complementary in the light of the effects of glacier retreat on stream temperatures. The following sections will feature a literature review of (1) physical controls on stream temperature and (2) proglacial lake dynamics, in order to

provide the context for the specific research questions that will be addressed in this thesis.

1.2 Literature review

1.2.1 Physical controls on stream temperature

Stream temperature varies diurnally and seasonally in response to natural cycles of solar radiation and streamflow. One or more components of the river heat budget may be modified by time-varying characteristics such as solar radiation, air temperature, relative humidity and wind speed, as well as site-specific characteristics such as amount of shade, temperature and discharge of groundwater and tributary inputs, and local topography. An understanding of the spatial and temporal variability of the processes that control stream temperature is an essential prerequisite to predicting stream temperature changes in any environment.

Energy budgets have been widely used to assist in understanding the processes that control stream temperature dynamics. The most successful studies have used on-site meteorological measurements and have been carried out in a variety of environments, including lowland and upland forested areas, low-gradient pasture, moorland and upland clearcuts (Brown, 1969; Evans et al., 1998; Webb and Zhang, 1999; Hannah et al., 2008). While most of these studies have used single measurements of meteorological variables, the importance of accounting for spatial variability within a reach has recently been recognised. Since net radiation arguably has the greatest influence on stream temperature (Webb and Zhang, 1999; Hannah et al., 2008), attempts have been made to model the spatial distribution of net radiation within stream reaches as influenced by topographic shading and canopy cover (Rutherford et al., 1997; Moore et al., 2005a; Guenther, 2007).

To the knowledge of the author, no stream energy budget study has been carried out in an alpine environment, which is surprising given that the high climate sensitivity of snowpacks and

glacier ice makes such areas particularly vulnerable to change (Hannah et al., 2007). As well as the thermal influence of dynamic source water contributions, including snow- and glacier ice-melt (Milner et al., 2001; Brown et al., 2006), alpine streams exhibit distinctive stream temperature dynamics due to (1) steep topography and (2) intense insolation caused by the lack of riparian shade and high elevation. Modelling the spatial variability in net radiation in alpine areas must account for the slope and aspect of the stream channel, as well as terrain shading. Stream temperature changes along a reach depend not only on the net heat transfer across the stream surface and bed, but also the width, depth and velocity of the flow. Width and depth can be highly variable and difficult to measure in steep, bouldery channels. A further effect of the steep channel gradient and irregular channel morphology is cascading flow, which could result in variable stream surface albedos. In addition, cascading flow would increase the effective water surface area in contact with the atmosphere, thus potentially enhancing the turbulent exchanges of sensible and latent heat. Previous stream heat budget studies have focused on relatively low-gradient channels, which can be well approximated as horizontal surfaces when modelling energy exchange at the water surface. No previous studies have considered the effects of non-horizontal surface and cascading flow on heat exchanges.

Despite the lack of energy budget studies focused on alpine streams, a number of researchers have demonstrated the heterogeneous nature of stream temperatures in such environments. Within the Rob Roy glacierised basin, New Zealand, Cadbury et al. (2008) attributed spatial variability in water column temperatures and overall modest warming rates of 0.6°C km^{-1} to (1) steep topography and a shaded southerly aspect, and (2) the incised river geomorphology. In this study, however, some riparian forest was present. In a glacierised catchment in Switzerland, Uehlinger et al. (2003) found that thermal heterogeneity between channels of an above-treeline glacial floodplain was greater than that observed along the main channel. While such studies of stream temperature patterns can provide qualitative information on the controlling factors,

only a study of stream heat budgets can provide a basis for making quantitative predictions of the temporal and spatial variability of stream temperatures and their response to environmental changes such as glacier retreat.

1.2.2 Thermal effect of a proglacial lake

Proglacial lakes can act as a heat source to through-flowing cold glacial melt water (Weirich, 1986; Uehlinger et al., 2003). The thermal effect of shallow, high-energy glacier-fed lakes is particularly complex due to the occurrence of strong katabatic winds, and the influence of high-volume, cool, sediment-laden inflows. While the heat content of most lakes is dominated by heat and momentum transfer across the surface (Chapra, 1997), advective heat transfers via the inlet and outlet play a more important role in many glacier-fed lakes. As well as heat content, outflow temperatures are also a function of the force of gravity acting on density differences within the lake. In low altitude, temperate lakes and reservoirs, temperature is typically the most significant determinant of water density (Mathews, 1956). In cold glacier-fed lakes, however, density differences due to sediment load often outweigh those due to temperature (Harris, 1976; Warren and Kirkbride, 1998).

Few studies appear to have simultaneously examined (1) the heat content of a lake and (2) controls on mixing and stratification within a lake, in the context of the thermal influence of the lake on through-flowing water. Most work focused on stream temperatures has merely reported inlet and outlet lake temperatures, with no mention of the physical processes responsible for the observed warming (Uehlinger et al., 2003; Robinson and Matthaei, 2007). While valuable insight can be gained by comparison of the physical characteristics of different study sites and observed inlet and outlet temperatures, quantification of controlling processes provides for a more rigourous basis with which to make future predictions on the thermal influence of glacier-fed lakes.

Most studies investigating the effects of glacier-fed sediment laden inflows on lake mixing have been carried out in deep, well stratified proglacial lakes (Gustavson, 1975; Chikita et al., 1996; Gilbert and Butler, 2004). Sturm and Matter (1978) went beyond simply identifying turbidity currents by proposing a three-mode conceptual model featuring over-, under- and inter-flows in deep, stratified glacial lakes with high sediment laden inflows. Overflows would occur when the density of inflowing water was less than that of the lake, underflows when the density of inflows was greater than that of the lake, and interflows when the inflow density is the same as that of the lake water. While modifications to the mixing model have been proposed for shallow proglacial lakes (Gilbert and Shaw, 1981; Smith et al., 1982), by far the most comprehensive study was carried out by Weirich (1986), which examined the occurrence of turbidity currents in Expectation Lake in southeastern British Columbia. The lake had a mean depth of approximately 5 m, surface area of 240,000 m^2 and featured a single inflow and outflow channel. Despite persistent isothermal conditions throughout the summer, underflows or overflows were observed depending on the sediment content of the inflow, which in turn was dependent upon the inflow discharge. Among other reasons, the lack of thermal stratification was attributed to (1) the fact that temperature has little control on density in cold lakes, (2) particularly effective wind-driven mixing, and (3) the mixing effect of underflows. Where inflows were of equal density to the lake water, homopycnal flows were reported, whereby rapid mixing and dispersal of suspended materials occurs as water enters the lake. It appears, therefore, that mixing in a shallow, high energy proglacial lake should be controlled primarily by a threshold controlled by the inflow discharge.

It is not unusual to find contrasting temperatures and temperature patterns in neighbouring lakes in similar contexts. For example, in a study of multiple ice-contact lakes in Mount Cook National Park, New Zealand, Warren and Kirkbride (1998) observed distinct thermal stratification in Hooker Lake and consistent isothermal conditions in nearby Maude Lake and

Godley Lake. Note that all of the lakes in the study occupied similar glacio-geomorphological settings. Frequent variations in mixing and stability over time in a single proglacial lake have not been reported in the literature, other than the tendency of Expectation Lake (Weirich, 1986) occasionally to stratify for short periods of time. The correct balance between surface energy exchanges and the volume and sediment load of inflows might result in proglacial lakes that remain close to a threshold, thus displaying complex cycles of mixing and stratification along with associated temperature variations.

As well as the extent of lake mixing, the heat content of a lake is crucial determinant of outflow temperatures. Heat content can be measured using a single vertical temperature profile, and expressed in units of energy normalised by the lake surface area (Wetzel, 1975). Heat content can also be modelled based on surface exchanges and the effects of inflows and outflows. Many researchers have used this comparison to gain insight into the dominant processes controlling lake temperatures at sub-diel, diel and longer timescales (Gibson and Stewart, 1973; Schertzer, 1978; Frempong, 1983; Potts, 2004). Few studies, however, have focused on small lakes, and even fewer on proglacial lakes. Given that the total heat content only has limited applicability in the interests of outflow temperatures (which are also dependent on the mixing of lake water), there is a clear need for studies that incorporate both an energy budget analysis of the heat content of the lake, as well as observations of the mixing effects of turbidity currents in proglacial lakes.

1.3 Research objectives

This research was motivated by three broad objectives, as listed below.

1. To characterize the thermal processes in a proglacial lake and the effects on alpine stream temperature, including (a) the relative roles of heat transfer by advection and vertical

exchanges at the lake surface, (b) the effects of mixing on water temperature profiles, and (c) the relation between lake temperature profiles and outflow temperatures.

2. To investigate heat transfer processes for a steep proglacial alpine stream with cascading flow, specifically (a) the effects of topographic shading and variable slope and aspect on net radiation, (b) the effect of cascading, frothy flow on energy exchanges, and (c) the effect of varying stream discharge on downstream warming.

3. To use the process knowledge generated by objectives 1 and 2 to generate hypotheses about the effect of future glacier retreat on alpine stream temperature regimes.

1.4 Thesis outline

Chapter 2 provides a description of the study area, description of the field measurements, and details of the methods of analysis and model development. The results in chapter 3 are divided into two sections, one corresponding to the lake study and the other to the stream study. Chapter 4 discusses the applied models for each part of the study and ends with an attempt to synthesise findings between the two components of the study. Chapter 5 concludes by summarising key findings and suggesting a direction for future research in the light of what has been found.

Chapter 2

Study area and methods

2.1 Study Area

This study focused on a proglacial lake and stream located below Place Glacier. Place Glacier is located 140 km north of Vancouver in the southern Coast Mountains, British Columbia, Canada. Local topography is dominated by U-shaped valleys fed by steep tributary streams, headed by cirque basins. The treeline is at around 1600 m. Mean annual precipitation at the valley bottom is between 750 and 1000 mm. Winter precipitation is between 1500 and 2500 mm. The hydrologic regime consists of low winter flows as most of the precipitation falls as snow, with high flows during the spring-summer melt season. Occasional rain events in autumn and winter also generate high flows.

Place Glacier has been monitored for mass balance since 1965. Between 1969 and 1984, Water Survey of Canada monitored streamflow at a weir just below the glacier terminus. UBC researchers have maintained a gauging station on Place Creek where it reaches Poole Creek in the valley bottom since 1997. Place basin faces northwest and is 13 km^2 at the valley bottom gauging site. The area of Place Glacier diminished from 4.0 km^2 in 1965 to 3.4 km^2 in 2001. This retreat led to the formation of two proglacial lakes, the largest of which (Place Lake) formed in the 1970s and flows directly into Place Creek. Outflow from Place Glacier discharges into the upper lake before flowing into Place Lake. The lakes are connected by a short, steep stream reach. Place Lake is approximately 70,000 m^2 (0.07 km^2) in area, and is at 1830 m a.s.l. It has

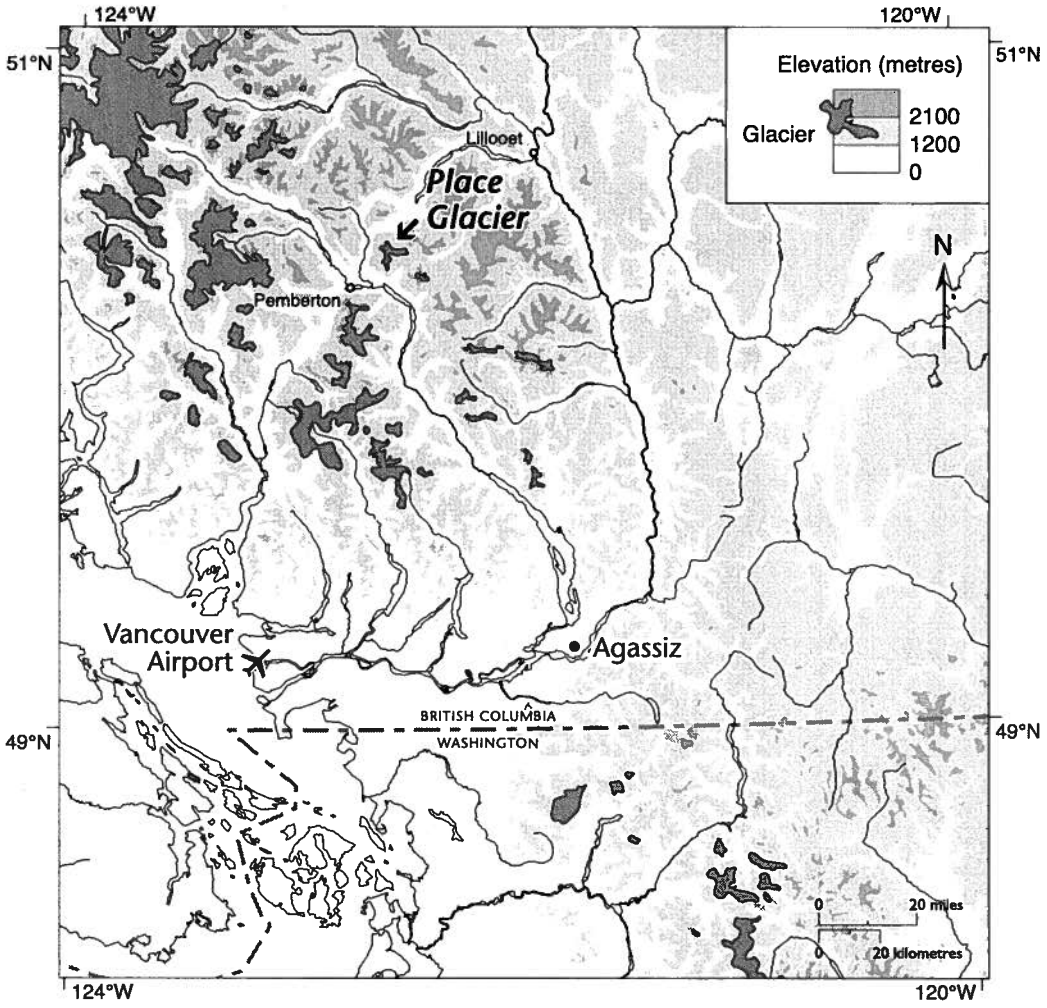

Figure 2.1: Map showing location of study area (adapted from map provided by R.D. Moore).

a maximum depth of about 12 m. Place Lake features two small islands (each < 100 m^2) and the outflow and inflow are positioned to the north and south, respectively. Below Place Lake, Place Creek flows for approximately 1000 m through two alpine cirque basins connected by a

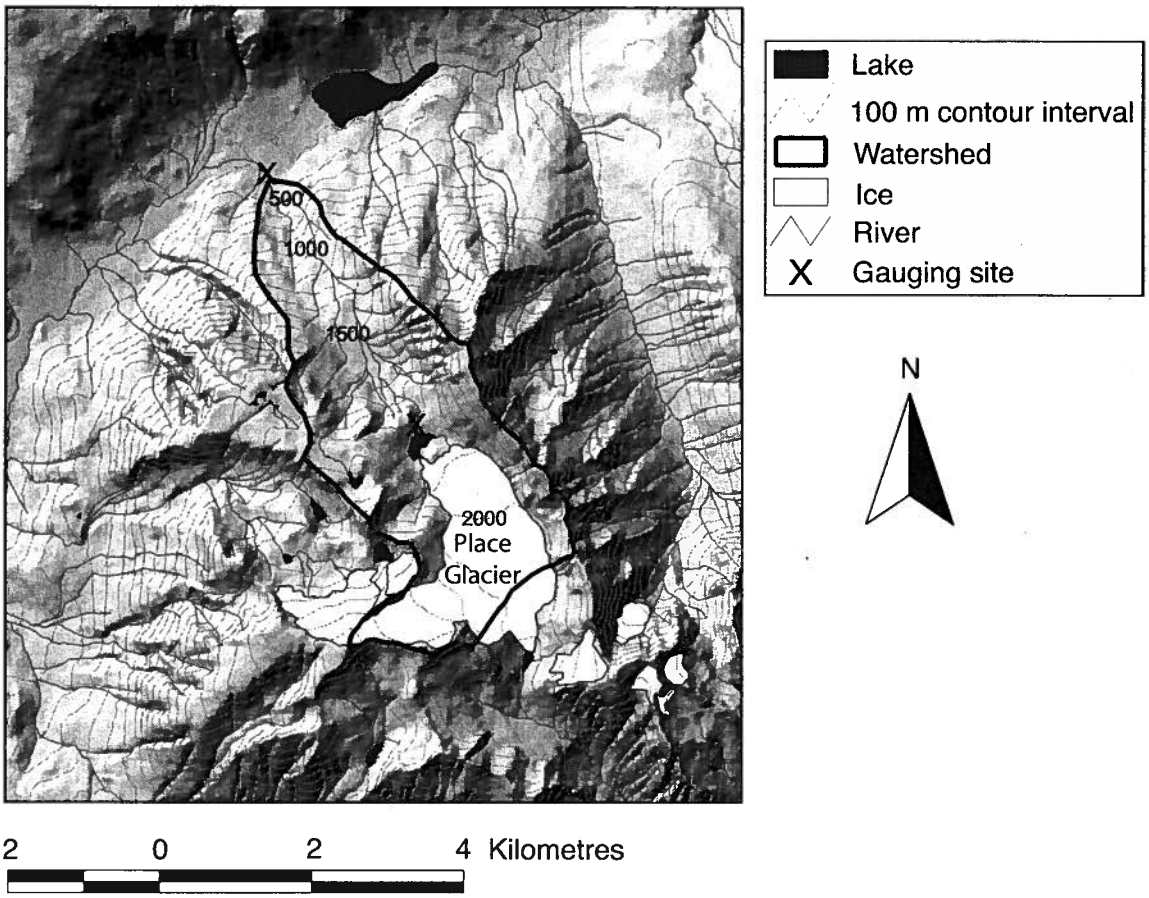

Figure 2.2: Map of study area (adapted from map provided by R.D. Moore).

steep headwall. Place Creek penetrates the treeline at 1560 m a.s.l. and eventually flows into a steep hanging valley. The above-treeline reach of Place Creek has no perennial tributaries. Large boulders dominate the channel morphology in the alpine and the channel gradient is variable, resulting in channel widths ranging from 4 to 12 m. In the lower-gradient section of each of the two alpine cirque basins, the stream becomes braided for a short distance.

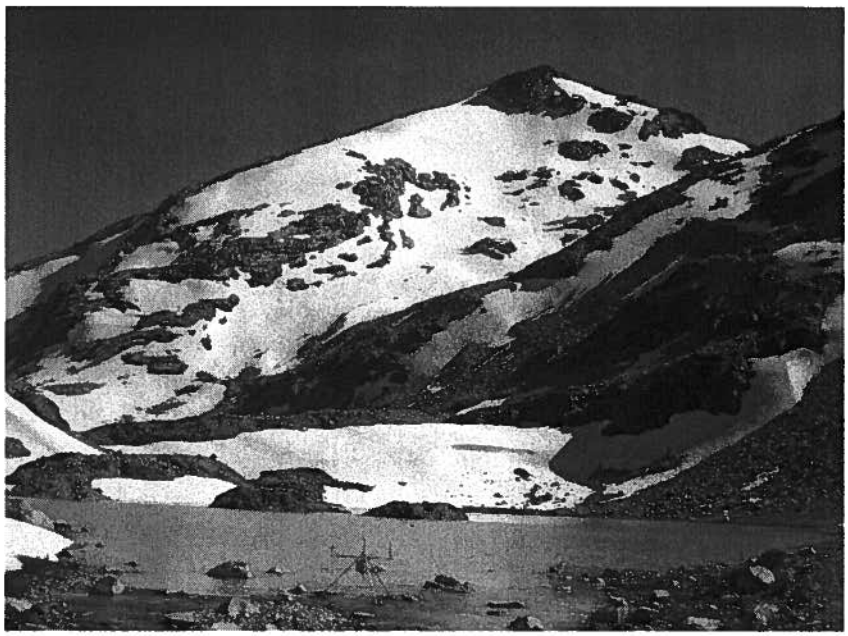

Figure 2.3: Place Lake and Place Lake Meteorological Station. Inflow is at centre back and outflow in foreground.

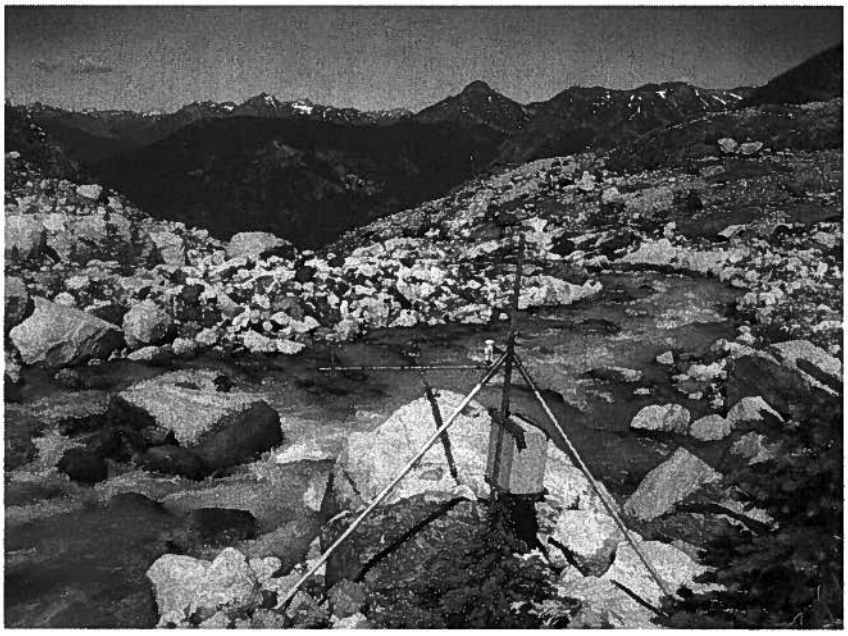

Figure 2.4: Place Creek and Place Creek Meteorological Station.

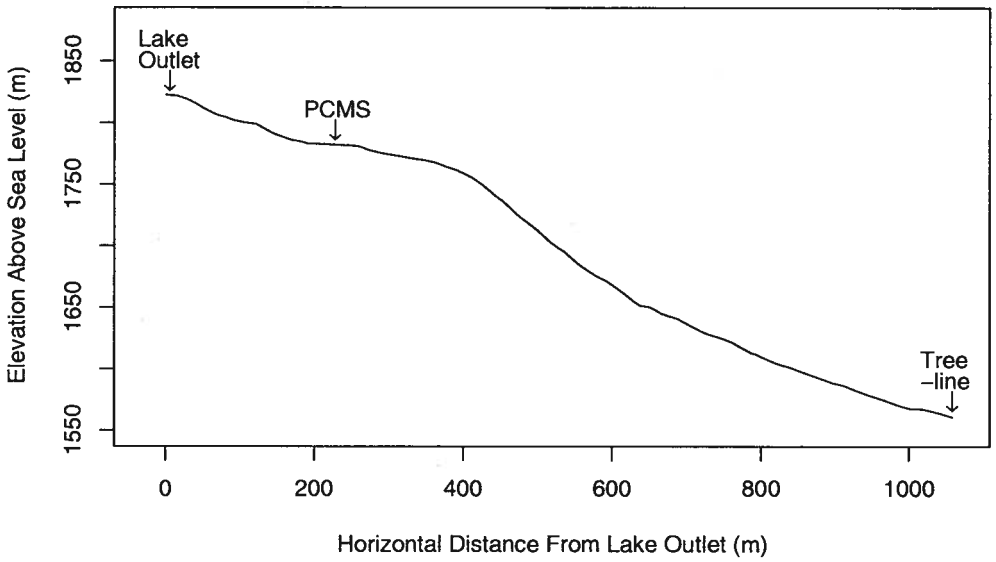

Figure 2.5: Long profile of Place Creek from Place Lake outlet to the treeline

2.2 Data collection and processing

2.2.1 Water temperature measurement

Due to heavy snow accumulation and late melting in 2007, field investigations at Place Lake and in the upper section of Place Creek were limited to the months of August and September. At the point of maximum depth (PL1 in Figure 2.6), a rope attached to a buoy and weight was used to secure Onset Tidbit v2 temperature loggers (accuracy $\pm 0.2°C$) at 8 depths (0, 0.5, 1, 2, 4, 6, 8 and 10 m below the water surface). All Tidbit loggers used in this study were programmed to record water temperature every 10 min.

Tidbit loggers were installed at four locations: the inflow and outflow of Place Lake, 150 m downstream of the outflow of Place Lake and at the treeline (900 m downstream of Place

Lake). Locations correspond to the four sites shown in Figure 2.6: Inflow, PLMS, PCMS and Treeline. Each logger was housed in a piece of white PVC piping which was anchored to the stream bed with a rock gabion and tied to a second anchor on the stream bank using heavy duty clothesline. The system ensured that loggers were not moved during high flows, were not in contact with the stream bed (which may be at a different temperature to ambient water temperature) and were not exposed to direct solar radiation during low flows.

Table 2.1: Instrument specifications

Parameter	Notation	Sensor	Range	Accuracy
air temp	T_a	Rotronic HC-S3	-30 to +60°C	±0.2°C
rel humidity	RH	Rotronic HC-S3	0-100%	±1.5% @ 23°C
net rad	Q_*	Kipp & Zonen NR-lite	0.2 - 100 μm	$-1\%/\text{ms}^{-1}$
		-30 to +70°C	0.12%/°C	
incident short	$K_\downarrow$	Kipp & Zonen CM6B	0.3 - 2.8 μm	$-1\%/\text{ms}^{-1}$
incident long	$L_\downarrow$	Kipp & Zonen CGR3	0.3 - 2.8 μm	$-1\%/\text{ms}^{-1}$
water temp	T_w	Onset UTBI-001	-20 to +70°C	±0.2°C
wind speed	u	MetOne 014a	0 - 45 ms^{-1}	±0.11 ms^{-1}
			[stall speed: 0.45 ms^{-1}]	
water level	*stage*	Van Essen DI 241	0-9 m	±0.1% FS
		-20 to +80°C	±0.1°C	
baro pressure	*baro*	Van Essen DI 250	0-1.5 m	±0.3% FS
		-20 to +80°C	±0.1°C	

2.2.2 Meteorological data

Wind speed, relative humidity, air temperature and water temperature were measured at the outflow of Place Lake (PLMS) every 10 s and averaged every 10 min (Figure 2.3). Instruments (Table 2.1) were attached to a Campbell Scientific CR10X datalogger and mounted on a tripod approximately 1.5 m above the water surface.

A second climate station (Figure 2.4), at PCMS (elevation 1780 m a.s.l), recorded net radiation in addition to the variables at the Place Lake station. Instruments were mounted on an aluminium frame that was extended over the channel approximately 1 m above the water

Figure 2.6: Aerial photograph of study area with highlighted stream channel and lake perimeters. Sampling sites are shown as black circles (photo courtesy of Eric Schiefer)

Table 2.2: Sampling design

Site	Data Collection	Notes
PM3	$K_{\downarrow}$	glacier site
RIDGE	$L_{\downarrow}$	open site
INFLOW	T_w	limited to 23 Aug - 16 Sept
PL1	T_w [depths: 0,0.5,1,2,4,6,8,10]	
PL2	*Stage Baro*	
PLMS	u RH T_a T_w Q	Q spot measurement
PCMS	Q_* u RH T_a T_w	
TREELINE	T_w	

surface. A tripod housing a Campbell Scientific CR10X datalogger was erected on the bank. The frame was secured to a boulder with screws cemented into the rock surface. The site was selected due to the presence of a large frothy pool that was deemed to represent general water surface conditions in the alpine reach.

Open site measurements of incident shortwave and longwave radiation were obtained from a climate station located on Place Glacier (PM3) and on a high ridge above Place Lake (Ridge), respectively.

Air temperatures for 2007 recorded at Pemberton Airport (approx. 30 km to the south-west) were obtained from the Environment Canada National Climate Archive. Snowpack water equivalent data for the Tenquille Lake snow course, 25 Km NW of Place Glacier, were obtained from the B.C. Ministry of Environment.

2.2.3 Discharge measurement

Stage was measured at the perimeter of Place Lake (PL2) using a Van Essen Diver housed in a stilling well, anchored to a large boulder at the lake shore. The Diver was programmed to measure water level and water temperature every 2 min, and was downloaded or replaced at approximately 22-day intervals. Barometric pressure was measured every 2 min using a Van Essen Baro housed in PVC pipe, sealed at the top to keep out moisture, and secured to a

boulder.

For steep, highly turbulent streams that experience high flows, slug injection using salt dilution is a well-tested stream gauging method (Moore, 2005a). Dry salt injection is arguably preferable when working in steep terrain as the procedure takes less time and requires less bulky equipment. Beyond the nature of the injection itself, dry salt injection only differs from salt-in-solution in the calibration procedure (outlined below). The dry salt injection method was tested against the salt-in-solution method during medium flows at Place Creek. Consecutive measurments showed less than 1% variation.

Boxes of salt were stored and transported in sealed bags to prevent leakage and the empty boxes were returned to the lab for weighing. For the dry salt method, a known mass of Sifto table salt (purity 99.9%), usually 1 kg, was injected as a slug (for salt-in-solution, the same mass was dissolved in a known volume of stream water, usually 6 L). The mass of salt was chosen based on the magnitude of flows and background Electrical Conductivity (EC). EC was measured between 60 and 100 m downstream of the injection point to record the timing and magnitude of the passing salt wave. The gauging reach was selected through field tests to ensure that complete lateral mixing occurred by the time the salt approached the observation point. It was found that short reaches resulted in inadequate resolution of the recorded salt wave, and that lengthy reaches resulted in excessive longitudinal dispersion and undetectable changes in EC. Reaches were avoided that lacked sufficient meanders or pinch points, had significant backwater areas, or displayed channel braiding.

Field calibration was carried out on-site for each non-consecutive discharge measurement. For the salt-in-solution method, the calibration solution was made by adding a known volume of the injection solution (5 or 10 mL) to 1 L of stream water. For the dry salt method, the calibration solution was made by adding a known mass of salt (approximately 1 g, pre-weighed and stored in dry sample bottles) to 1 L of stream water. For each technique, successive

increments of the calibration solution (5 or 10 mL depending on EC range of the observed salt wave) were added to a second known volume of streamwater (1 L), and EC was recorded after each addition. The slope of this relation is used in the calculation of discharge and has different units depending which the injection method used. For the salt-in-solution method, the slope, k_s represents the relation between relative concentration and EC. For dry injection, the slope, k_d, represents the relation between mass concentration and EC. For the salt-in-solution method, discharge was calculated as:

$$Q = \frac{V}{k_s \Delta t \sum [EC_t - EC_{bg}]} \tag{2.1}$$

where Q = stream discharge (m^3s^{-1}), V = volume of salt solution injected (m^3), EC_t = electrical conductivity (μS/cm) at time t, EC_{bg} = the background EC and k_s = the calibration constant for salt-in-solution (cm/μS). For the dry salt method, discharge was calculated as:

$$Q = \frac{M}{\Delta t \sum [k_d (EC(t) - EC_{bg})]} \tag{2.2}$$

where M = mass of salt injected (kg) and k_d = the calibration constant for dry salt injection.

A stage-discharge rating curve was established for the lake outlet site using discharge measurements at a range of flows. The following relation was fitted to the data using nonlinear least squares (NLS) regression:

$$\log Q = 1.5174 \cdot \log (S - 1.9665) \tag{2.3}$$

where S = stage (cm). The rating curve and data are shown in Figure 2.7. For the Place Lake outflow, the standard error of the estimate (SEE) was 0.0244 m^3s^{-1} (2% of the mean calculated discharge), indicating a reasonable prediction of discharge from stage.

The stage record was modified in four ways. Firstly, on 14 occasions over the six week study

period, outliers were removed where data points severely mismatched the local trend. Secondly, parts of the dataset the record from the Van Essen Baro instrument did not resemble data from other instruments deployed further downstream. This error was attributed to instrument malfunction. For these cases, the barometric pressure was modelled by means of a simple linear regression using a reliable section of the Place Lake Baro record. Thirdly, a step change in stage was experienced during the transfer of two identical instruments (transfers were necessary due to low memory capacity). A shift correction was applied to remove this step change. Finally, the stage record for Place Lake was cleaned using a 101 point binomial filter to reduce fine scale variability that was believed to be caused by inadequate smoothing of waves by the stilling well.

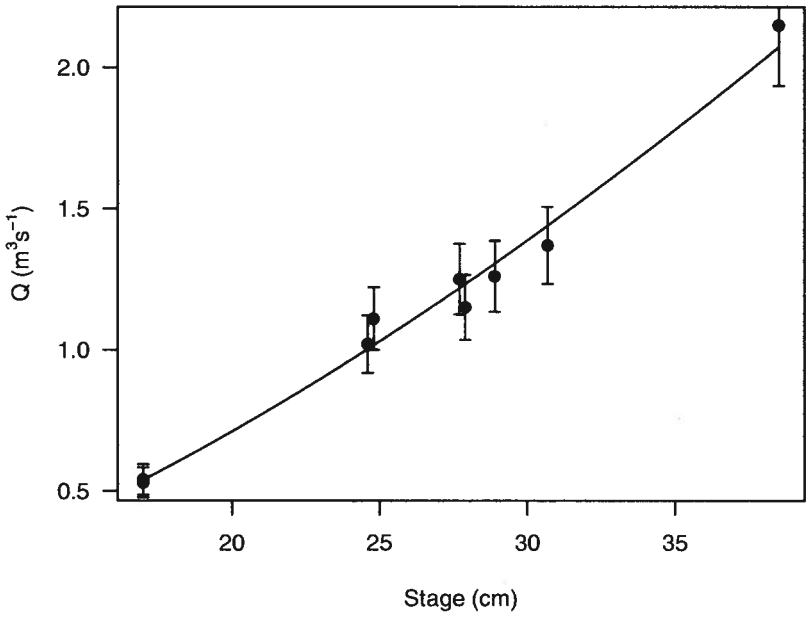

Figure 2.7: Place Creek stage-discharge rating curve. Error bars indicate ±10% of the calculated discharge.

2.2.4 Calculation of lake inflow

The inflow discharge of Place Lake was calculated as:

$$q_i = q_o - \Delta V_l / \Delta t \tag{2.4}$$

where q_i and q_o = respective inflow and outflow discharge ($m^3 s^{-1}$), Δt = change in time (s), ΔV_l = the change in lake volume (m^3) over time, t, which can be calculated as:

$$\Delta V_l = \Delta S \cdot A_l \tag{2.5}$$

where, ΔS = the change in lake stage (m) and A_l = lake surface area (m^2).

2.3 Calculation of surface heat fluxes

The net energy exchange at the water surface (of both the lake and the stream), Q_n can be calculated as:

$$Q_n = Q_r + Q_e + Q_h \tag{2.6}$$

where Q_r = heat flux due to net radiation, Q_e = latent heat flux and Q_h = heat flux due to sensible heat transfer between the air and water. Note that positive heat flux values represent a gain of energy at the water surface. All energy exchanges have units of Wm^{-2}.

Net radiation was calculated as:

$$Q_* = K\downarrow - K\uparrow + \epsilon_w L\downarrow - L\uparrow \tag{2.7}$$

where $K\downarrow$ = incident solar shortwave radiation, $K\uparrow$ = reflected shortwave radiation from the surface, ϵ_w = emissivity of water, which was assumed to be 0.97 (Oke, 1987), $L\downarrow$ = incident longwave radiation $L\uparrow$ = longwave radiation emitted from the water surface.

2.3.1 Solar radiation

Incident solar shortwave radiation was measured at PM3. Reflected shortwave radiation from the lake surface was calculated as $\alpha K_{\downarrow}$, where α is the albedo of the water, which was assumed to be constant at 0.05 (Oke, 1987).

The spatial variability in solar radiation was modelled at Place Lake and along the alpine reach. The amount of solar irradiance reaching the water surface depends on (1) sun-earth geometry, (2) atmospheric conditions and (3) the influences of local topography and vegetation. It was assumed that the net effect of riparian vegetation was minimal given the alpine setting.

A 25 m resolution digital elevation model (DEM) was clipped to an area around the study site that included all influential topography. The lake and stream channel were delineated visually by overlaying the DEM with a digital aerial photograph. Data for x and y grid coordinates and elevation were extracted for 115 grid points in the lake and 38 points throughout the stream reach. Slope and aspect were also extracted for the alpine reach. Horizon angles for 10° interval ground azimuths (36 points) were computed from the elevation data. The sky dome was split into 10° azimuth by 1° zenith grid cells. A gap fraction, G_t, of 1 was applied to cells above the horizon and 0 to cells below the horizon for each grid point. Sky view factors were computed for each grid point in the lake as:

$$f_v = \frac{1}{\pi} \sum \left[G_t \cos\theta \sin\theta \right] \delta a \, \delta z \tag{2.8}$$

where f_v = sky view factor, G_t = gap fraction, θ = solar zenith angle (radians), δa = angular increment for the azimuth (radians), $\delta\theta$ = angular increment for the solar zenith (radians). Sky view factors throughout the stream reach were adjusted for the inclination of the channel, and were thus calculated as:

$$f_v = \frac{1}{\pi} \sum \left[G_t \cos i_s \sin \theta \right] \delta a \, \delta z \tag{2.9}$$

where i_s = the angle of incidence at the stream surface for radiation originating from each cell in the sky dome (radians), which was calculated at each of the 38 grid points along the alpine reach as:

$$\cos i_s = \sin \beta \sin \theta \cos (z - a) + \cos \beta \cos \theta \tag{2.10}$$

where, β = slope inclination from horizontal (radians), z = solar azimuth angle (radians) and a = slope azimuth angle (radians).

The local solar path (azimuth and zenith) for each day was calculated using equations from Iqbal (1983). Atmospheric transmissivity, τ, was computed as the ratio of measured open-site incoming solar radiation to computed potential extraterrestrial solar radiation, $K_{\downarrow pot}$, which was calculated as:

$$K_{\downarrow pot} = S \cos i_h \tag{2.11}$$

where S = solar constant (1367 Wm $^{-2}$) and i_h = the angle of solar incidence on the horizontal (equivalent to the solar zenith angle) (radians), which was calculated from the solar declination angle, the hour angle and the latitude of the site (see Iqbal (1983) for equations). The diffuse component of incident shortwave radiation, $K_{\downarrow dif}$ (Wm^{-2}), was computed from τ and $K_{\downarrow pm3}$ using equations from Erbs et al. (1982). For the lake, the direct component of incident shortwave radiation was then computed as:

$$K_{\downarrow dir} = K_{\downarrow pm3} - K_{\downarrow dif} \tag{2.12}$$

where $K_{\downarrow dir}$ = direct component of incident shortwave radiation (Wm^{-2}) and $K_{\downarrow pm3}$ = incident

shortwave radiation measured at PM3 (Wm^{-2}). For the stream, the direct component of incident shortwave radiation was adjusted to account for the sloping channel surface:

$$K_{\downarrow dir} = (K_{\downarrow pm3} - K_{\downarrow dif}) \cdot \frac{\cos i_s}{\cos i_h} \tag{2.13}$$

A solar terrain 'mask' was determined for each day at each point along the reach by comparing the horizon angle of the terrain to that of the solar zenith at the ground azimuth that corresponded with the solar azimuth (the gap fraction for the sky dome was effectively clipped to the solar path). If the solar zenith angle was greater than the complement of the horizon angle then the site was in sun and received direct beam radiation.

For both the lake and stream, modelled incident shortwave radiation was calculated as:

$$K_{\downarrow} = K_{\downarrow dir} G_t + K_{\downarrow dif} f_v \tag{2.14}$$

Reflected shortwave radiation from the surface was calculated as:

$$K_{\uparrow} = \alpha K_{\downarrow} \tag{2.15}$$

where α = albedo of the water surface, which was assumed to be 0.05 at the lake. Because it was hypothesised that the albedo of the stream would increase with discharge due to the increased frothiness of the flow, it was modelled as:

$$\alpha = \alpha_0 + jq^k \tag{2.16}$$

where α_0 was assumed to equal 0.05, and j and k were coefficients fitted using nonlinear least squares (NLS) regression, using the nls function in R (version 2.6.0).

2.3.2 Longwave radiation

Incident longwave radiation was measured at the Ridge site. For the radiation models at the lake and the stream, incident longwave radiation was calculated as:

$$L_{\downarrow} = L_{\downarrow rs} f_v + (1 - f_v)\, \epsilon_t\, \sigma {T_a}^4 \tag{2.17}$$

where $L_{\downarrow rs}$ = Ridge site measured incident longwave radiation (Wm^{-2}), ϵ_t = emissivity of the terrain, which was assumed to be 0.95 (Oke, 1987), σ = Stefan-Boltzmann constant (5.67×10^{-8} W m^{-2} K^{-4}), T_a = air temperature (K). Longwave back radiation from the surface of both the lake and the stream was calculated as:

$$L_{\uparrow} = \epsilon_w \sigma T_s^4 \tag{2.18}$$

σ = the Stefan-Boltzmann constant (5.67×10^{-8} W m^{-2} K^{-4}) and T_s = water surface temperature (K).

2.3.3 Latent and sensible heat fluxes

The heat flux due to evaporation and condensation can be calculated using an adapted form of the Penman-type equation as presented by Webb and Zhang (1997) :

$$Q_e = 285.9\,(0.132 + 0.143u)\,(e_a - e_w) \tag{2.19}$$

where u = wind speed measured at a height of about 1 m above the water surface (ms^{-1}), e_a and e_w = vapour pressures of the air and water, respectively (kPa), and the constants account for the applied unit conversions, physical constants such as the latent heat of vaporisation, and empirical constants in the Penman equation. The vapour pressure of the water surface can be calculated as (Stull, 2000):

$$e_w = 0.611 \cdot exp\left[5423\left(\frac{1}{T_0} - \frac{1}{T_w}\right)\right] \tag{2.20}$$

where $T_0 = 273.2$ K, T_w = water temperature (K). The vapour pressure of the air was calculated as:

$$e_a = (RH/100) \cdot e_s \tag{2.21}$$

where RH = relative humidity and e_s = saturation vapour pressure of the air (kPa), calculated as:

$$e_s = 0.611 \cdot exp\left[5423\left(\frac{1}{T_0} - \frac{1}{T_a}\right)\right] \tag{2.22}$$

where T_a = air temperature (K).

The sensible heat flux can be calculated as:

$$Q_h = [\gamma\,(T_a - T_w)\,/\,(e_a - e_w)]Q_e \tag{2.23}$$

where T_a = air temperature (°C) and γ = the psychrometric constant (kPa°C^{-1}) which was calculated as:

$$\gamma = 6.6 \times 10^{-4} \cdot P \tag{2.24}$$

where P = atmospheric pressure (kPa).

2.4 Calculation of lake heat budget

The total heat content of the lake at any time can be calculated as the sum of the heat content of individual layers associated with each temperature measurement:

$$H_t = \sum H_j \tag{2.25}$$

where H_t = the total heat content per unit area of the lake ($\mathrm{MJm^{-2}}$) and H_j = the heat content of layer j of the lake ($\mathrm{MJm^{-2}}$):

$$H_j = \frac{A_j D_j C\,(T_j - T_r)}{A_l} \tag{2.26}$$

where A_j = the surface area of layer j ($\mathrm{m^2}$), D_j = the depth of layer j (m), T_j = the temperature of layer j (°C) and T_r = the reference temperature (see below) (°C).

Heat content must be defined with respect to a reference temperature, such that when $T = T_{ref}$, $H_l = 0$ (Potts, 2004). A common choice of T_r for temperate lakes is 4°C (the temperature of maximum density) so that $H_l < 0$ implies reverse (winter) stratification and $H_l < 0$ implies summer stratification. The short study period and relatively low temperatures of Place Lake mean that a T_r of 0°C is more suitable.

2.5 Lake modelling

The thermal behaviour of the lake was computed using three models of varying complexity. The first assumed that the lake behaved as a Completely Stirred Tank Reactor (CSTR). The second model assumed minimal heat exchange across the epilimnion and also that advective heat exchanges were negligible. The third and most complex model, DYRESM, modelled vertical heat exchange across different horizontal layers of the lake to compute a vertical temperature profile over time.

2.5.1 CSTR model

For a completely mixed lake, the change in water temperature over time can be calculated as:

$$\frac{\delta T}{\delta t} = \frac{H_i - H_o - H_e + Q_n \cdot A_l}{V_l \cdot C} \tag{2.27}$$

where δT = the change in lake temperature (°C), δt = the time interval used, H_i and H_o = advective energy associated with the inflow and outflow (W m^{-2}), H_e = advective energy associated with water lost by evaporation (W m^{-2}), A_l = lake surface area (m), V_l = lake volume (m^3) and C = heat capacity of water ($Jm^{-3}s^{-1}$). Equation 2.27 assumes that groundwater discharge into the lake is negligible. The advective energy associated with the inflow (or outflow) (Wm^{-2}) can be calculated as:

$$H_i = q_i \cdot C \cdot T_i \tag{2.28}$$

where q_i = the inflow (outflow) discharge (m^3s^{-1}) and T_i = inflow (outflow) temperature (°C). The advective energy associated with water lost by evaporation can be calculated as:

$$H_e = E \cdot C \cdot T_s \tag{2.29}$$

where T_s = water surface temperature (°C) and E = rate of evaporation from the lake surface (m^3s^{-1}), which can be calculated as:

$$E = \frac{Q_e \cdot A_l}{\rho \cdot L_v} \tag{2.30}$$

where ρ = density of water (kgm^{-3}) and L_v = latent heat of vaporisation (Jkg^{-1}), which can be calculated as:

$$L_v = 2.5 \times 10^6 - 2.386 \times 10^3 \cdot T_a \tag{2.31}$$

where T_a = air temperature (°C).

2.5.2 Epilimnion model

Given the distinct similarity between observed mid-lake and outflow temperatures, the following model assumes that no mixing occurs across the epilimnion of the lake. The input water temperature for the surface flux calculations was updated at each time step with the new modelled water temperature. The model is a simplification of Equation (2.27), in which the advective terms are ignored and the depth of the lake is adjusted to the estimated depth of the epilimnion:

$$\frac{\delta T}{\delta t} = \frac{Q_n}{CD_e} \tag{2.32}$$

where D_e = depth of epilimnion (m)

2.5.3 DYRESM

DYRESM (DYnamic Reservoir Simulation Model) is a one-dimensional numerical model for predicting the vertical distribution of temperature, salinity and density in lakes and reservoirs (Imerito, 2007). The lake is represented as a series of horizontal layers of uniform property but different thickness, which expand or contract as other layers move up or down to accommodate volume change. The surface area of each layer changes in accordance with the lake bathymetry. An important feature is the assumption of one dimensionality, which ignores lateral variations within layers. Indeed, lateral and longitudinal variations in density are often negligible in lakes and reservoirs (Moshfeghi et al., 2005). Mixing between layers is modelled by amalgamation of adjacent layers, and adjustments to layer thicknesses.

Exchanges of heat, mass and momentum across the surface of the lake are the main driving mechanisms for DYRESM. Meteorological input data, therefore, include measures of shortwave radiation, longwave radiation and air temperature, as well as estimates of sensible and latent heat and wind speed. Rainfall is a required input, but was assumed to be negligible here.

Table 2.3: DYRESM input parameters

Parameter	Data Source	Notes
T_a	Lake Met	
RH	Lake Met	
WS	Lake Met	
$K_{\downarrow}$	Open Site	
$L_{\downarrow}$	Open Site	
T_w	(1) Inflow	
	(2) Outflow - Lake Met	
	(3) Depth Profile	
q_o	Q5 guaging stn	
q_i	Calculated	
A_l	DEM derived	
$Bath$	Modelled from A_l	
T_w profile	Lake Tidbits	
T_i	measured / modelled	before 23 Aug, modelled from T_o using SLR
T_o	measured	

Additional parameters must characterise inflows and outflows in terms of discharge, water temperature, channel geometry and entry/exit height (referenced to the lake bed). Inflow discharge was modelled from the outflow discharge as demonstrated in Equation 2.4. Knowledge of the lake morphometry is required, but in the absence of bathymetric data, the lake was modelled as a parabolic bowl. Note that such an assumption may be responsible for errors given that the geometry of Place Lake is complex and features a small island in the south-eastern sector. An initial temperature profile with depth is required to drive the model, which was programmed to operate on an hourly timestep and was run for 47 consecutive days to cover the study period. Table 2.3 shows the sources of the data for each of the inputs required to run DYRESM. Figure 2.8 shows how the model operates; a simulation file is produced from 7 input files (the mixing component was ignored here), which is subsequently modified by the DYRESM model itself.

DYRESM was calibrated with the help of A. Forrest (Department of Civil Engineering,

University of British Columbia). Calibration focused on achieving adequate heat distribution throughout the water column and involved a single step in which the inflow was split such that those flows $> 120{,}000\ m^3d^{-1}$ were forced to enter the system at the bottom of the lake (mimicking plunging, sediment laden inflows) and those that were $< 120{,}000\ m^3d^{-1}$ were allowed to enter on the surface. Further discussion will be offered in Chapter 4. It should be noted that the application of this model is intended to be exploratory.

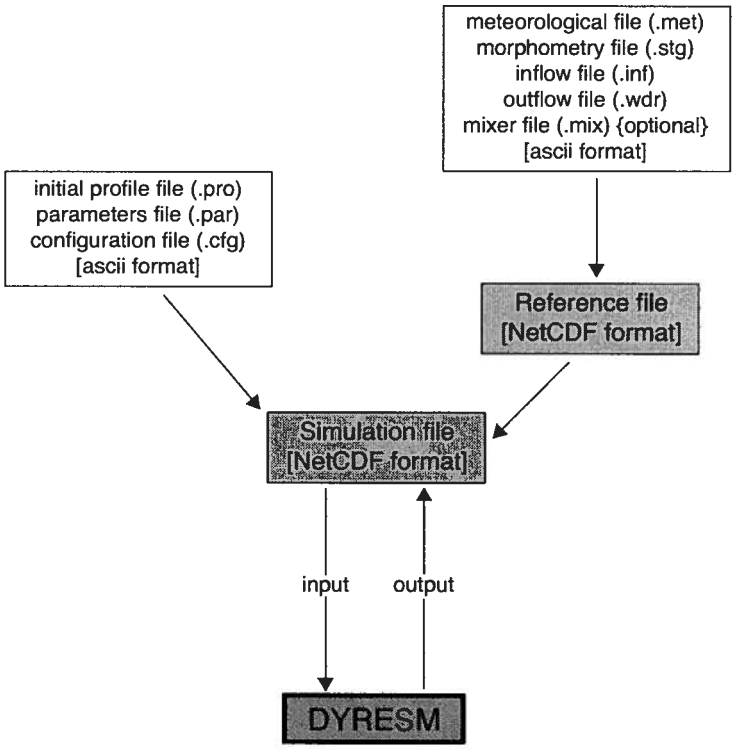

Figure 2.8: DYRESM simulation process in which 7 input files are required to produce the simulation file, which is then modified by the model program to produce an output simulation file which can be compared to observed data

2.6 Stream heat budget modelling

2.6.1 Description of models

Downstream temperature changes were modelled using four versions of a steady-state heat budget model. The models ignore longitudinal dispersion, heat inputs from precipitation, and the influence of lateral inflows, groundwater and hyporheic exchange.

The temperature change that occurs as a parcel of water flows downstream can be expressed as:

$$\Delta T = (L/C) \cdot (Q_* + Q_h + Q_e) \cdot w/q + g\Delta Z/C \tag{2.33}$$

where ΔT = downstream change in water temperature (°C), L = reach length (m), C = heat capacity of water ($\mathrm{Jm^{-3}{}^{\circ}C^{-1}}$), w = average channel width (m), q = discharge ($\mathrm{m^3s^{-1}}$), g = Earth's gravitational acceleration ($\mathrm{ms^{-2}}$) and ΔZ = change in elevation (m). The second term represents the warming due to frictional dissipation of potential energy.

Given that the channel width varies over both space and time, but cannot be measured accurately, the width term in Equation 2.33 was assumed to vary as a power function of discharge in the second model:

$$w = a \cdot q^b \tag{2.34}$$

where a and b are constants, with a representing the channel width at a flow of 1 $\mathrm{m^3s^{-1}}$. The function in Equation 2.34 can then be substituted for the width term in Equation 2.33:

$$\Delta T = (L/C) \cdot (Q_* + Q_h + Q_e) \cdot aq^{b-1} + g\Delta Z/C \tag{2.35}$$

A further modification can be made by multiplying the turbulent fluxes by a constant:

$$\Delta T = (L/C) \cdot \Big[Q_\star + c\,(Q_h + Q_e) \Big] \cdot a q^{b-1} + g\Delta Z/C \tag{2.36}$$

where c is a constant. This modification follows from the hypothesis that sensible and latent heat exchanges for cascading flow are greater than predicted from standard wind functions. A final version of the model allows the sensible and latent heat fluxes to vary independently:

$$\Delta T = (L/C) \cdot \Big[Q_\star + cQ_h + dQ_e \Big] \cdot a q^{b-1} + g\Delta Z/C \tag{2.37}$$

where d is a constant. The coefficients a, b, c and d were estimated by using NLS regression to maximise the agreement between predicted and observed ΔT. The four models are summarised in Table 2.4.

Table 2.4: Summary of alpine energy budget models. Note that all four models are driven by reach averaged air and stream temperatures, reach averaged modelled net radiation, and discharge as measured at the lake outlet

Model	Equation	Notes
1	$\Delta T = (L/C) \cdot (Q_\star + Q_h + Q_e) \cdot w/q + g\Delta$Z/C	Standard energy budget
2	$\Delta T = (L/C) \cdot (Q_\star + Q_h + Q_e) \cdot a q^{b-1} + g\Delta$Z/C	Parameterised width term
3	$\Delta T = (L/C) \cdot [Q_\star + c\,(Q_h + Q_e)\,] \cdot a q^{b-1} + g\Delta$Z/C	Optimised turbulent fluxes
4	$\Delta T = (L/C) \cdot [Q_\star + cQ_h + dQ_e] \cdot a q^{b-1} + g\Delta$Z/C	Optimised turbulent fluxes

2.6.2 Calculation of goodness-of-fit statistics

The Root Mean Squared Error (RMSE) and Mean Average Error (MAE) are among the best overall measures of model performance as they summarise the mean difference in the units of the observed and predicted variables (Willmott, 1982). The main difference is that the MAE

is less sensitive to extreme values than the RMSE. For each of the NLS models, the RMSE and MAE were calculated as:

$$\text{RMSE} = \left[N^{-1} \sum_{i=1}^{N} (P_i - O_i)^2 \right]^{0.5} \tag{2.38}$$

$$\text{MAE} = N^{-1} \sum_{i=1}^{N} |P_i - O_i| \tag{2.39}$$

where N = the number of cases, P_i = model predicted variable, O_i = observed variable.

The Mean Bias Error (MBE) is the difference between the mean of the model predicted variable and the observed variable and was calculated as:

$$\text{MBE} = N^{-1} \sum_{i=1}^{N} (P_i - O_i) \tag{2.40}$$

Akaike's Information Criterion (AIC) is another popular model comparison statistic (lower values indicate a better fit) that introduces a penalty for the number of parameters in the model. The AIC was provided by the output of the nls function in R (version 2.6.0), and is calculated as:

$$\text{AIC} = 2k - 2ln(L) \tag{2.41}$$

where k is the number of parameters in the statistical model and L is the maximised value of the likelihood function for the estimated model. As a final means of comparison for the NLS models, the pseudo R^2 was calculated as:

$$I^2 = \frac{\text{(SSY - SSE)}}{\text{SSY}} \tag{2.42}$$

where I^2 = the pseudo R^2, SSE = sum of squares error and SSY = sum of squares of the predicted variable, for which an adjusted value was calculated as:

$$\text{SSY} = \sum_{i=1}^{N} P_i^2 - \left[\sum_{i=1}^{N} P_i \right]^2 N^{-1} \tag{2.43}$$

Chapter 3

Results

3.1 Overview of study period

Snow accumulation preceding the 2007 field season was 43% greater than the long-term average at Tenquille Lake (Figure 3.1). Unfortunately, the 2007 Pemberton Airport climate record was incomplete, and thus no reliable precipitation or air temperature data (apart from August and September) were available for the entire summer of 2007. Air temperatures during 2007 were similar to the long-term average at Vancouver International Airport, although July was 7%

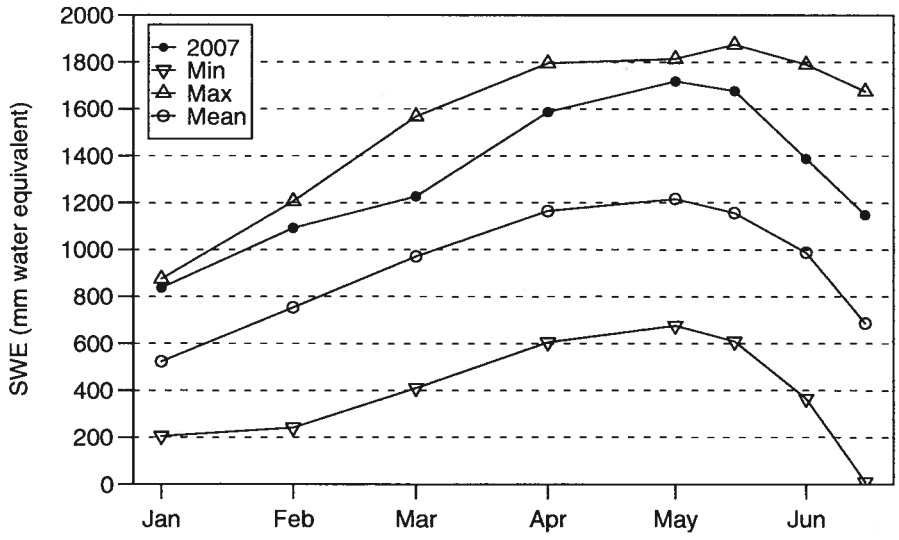

Figure 3.1: Snowpack water equivalent at the Tenquille Lake snow course, including observed values for 2006 and 2007, as well as the minimum, maximum and mean values for the period of record (Source: B.C. Ministry of Environment Historical Snow Survey Data)

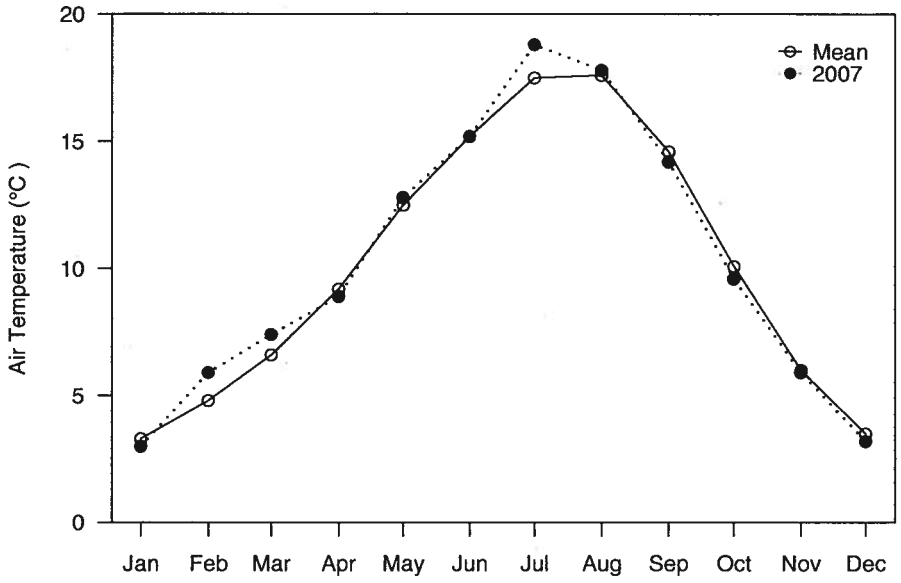

Figure 3.2: Vancouver International Airport long-term average (1971-2000) and 2007 mean monthly air temperatures

warmer in 2007 (Figure 3.2).

The large snowpack of 2007 and ice cover on Place Lake prevented safe access to the alpine area before the end of July. Bad weather prevented access after 18 September. Place Lake inflow temperatures were not recorded until 23 August. Gaps in the Pemberton Airport air temperature record in Figure 3.3 are due to missing data.

A continuous record of discharge was obtained from 20 July to 18 September 2007 (Figure 3.3). This record was too short to show a clear seasonal fluctuation. Based on observations at the valley bottom in 2000 and 2001, discharge typically increases in mid-May from near 0 m^3s^{-1} to around 2 m^3s^{-1} in early July (Richards and Moore, 2003). Seasonal high flows of up to 4 m^3s^{-1} often occur in early August (Moore and Demuth, 2001). The deep snowpack and lack of a sustained period of high air temperatures in August and September explain the lack of high flows in 2007. Figure 3.3 also shows incident shortwave radiation at Place Glacier,

stream temperatures at three selected sites and air temperatures at Place Lake and Pemberton Airport.

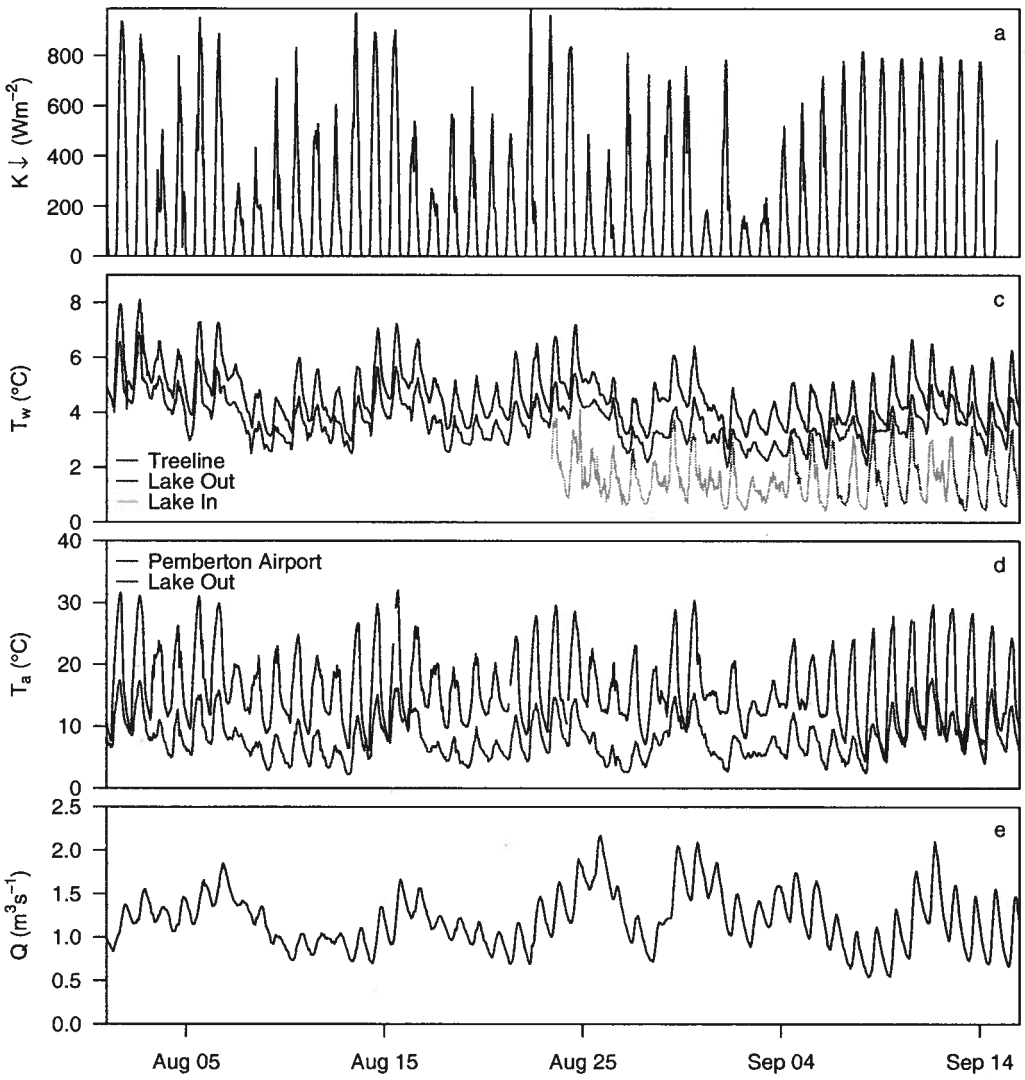

Figure 3.3: Time-series of (a) incident shortwave radiation at PM3, (b) stream temperature, (c) air temperature and (d) discharge at the lake outlet

3.2 Place Lake

3.2.1 Observed temperature trends

Place Lake had a consistent warming effect of 1-3°C (average 1.8 °C) on through-flowing water. Inflow temperatures varied diurnally by up to 3°C, whereas mid-lake surface and outflow temperatures fluctuated by less than 2°C. This difference in diurnal amplitude was particularly apparent on clear sky days. During the six week study period, surface temperatures in the middle of Place Lake were consistently similar to outflow temperatures, implying that the outflow was dominated by surface water (Figure 3.4).

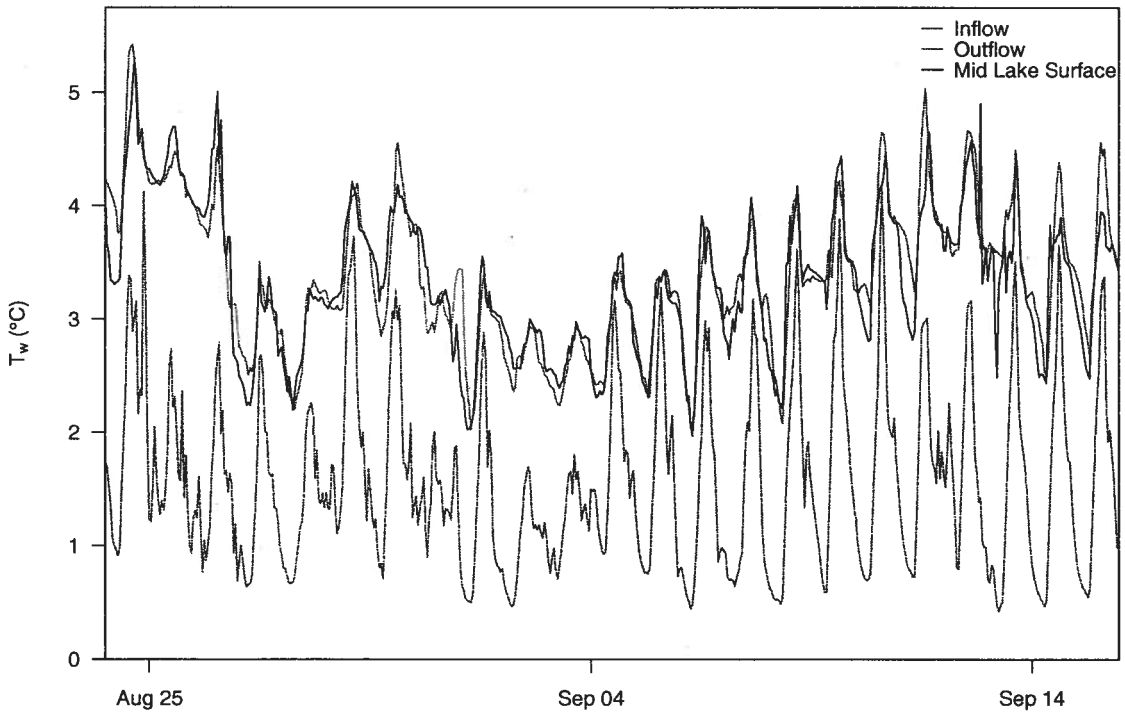

Figure 3.4: Place Lake inflow, outflow and mid lake surface temperatures between August 24th and September 16th

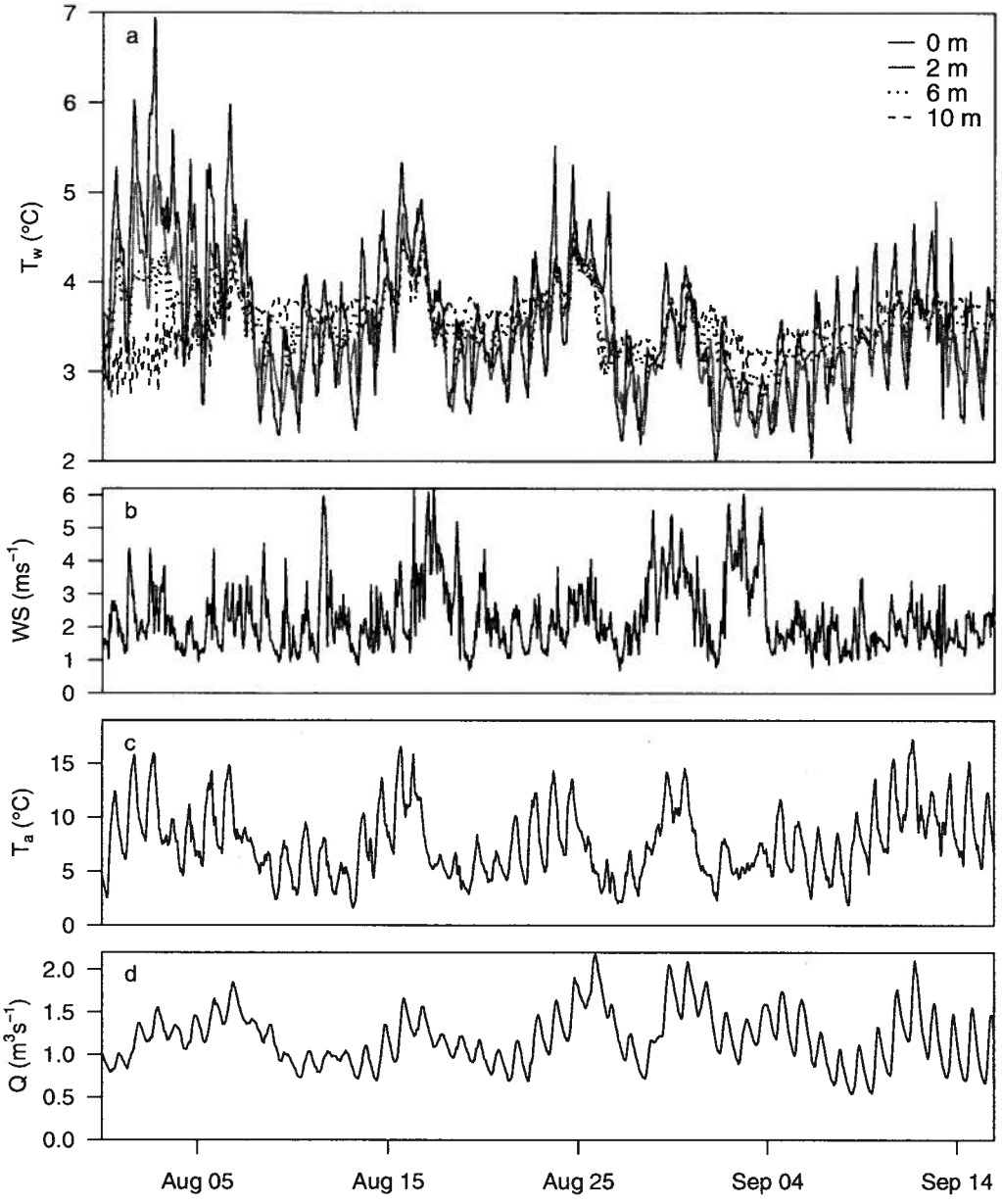

Figure 3.5: Hydrometeorological conditions at Place Lake (a) Shows mid-lake temperatures at selected depths. (b), (c) and (d) show wind speed, air temperature and discharge at the lake outlet, respectively

Figure 3.5 shows a time series of lake temperatures at selected depths, along with wind speed, air temperature and discharge at the lake outlet. Subsurface temperatures generally fluctuated around 3.5°C. While temperatures at all depths displayed similar synoptic scale (1 to 7 days) trends, diel fluctuations varied between depths and over time. The highest surface temperatures, of approximately 7°C, were recorded at the beginning of August. On the diurnal timescale, the lake temperatures indicated more complete mixing during the day and stratification during the night. On the majority of days, surface water cooled to a temperature below that of deeper water during the night. Four periods of higher air temperatures and discharge, on around the 16, 26, 30 August and 12 September, were correlated with higher lake temperatures and more complete mixing throughout the water column (seen by similar temperatures at all depths). While the first and third of these periods were associated with higher wind speeds, the other two were not. Synoptic scale troughs in the air temperature record (which occurred a few days prior to each of the four peaks) were associated with stratification characterised by warmer water overlying cooler water. A transition in lake stability occurred on around 7 August, when the water column became fully mixed for the first time during the study period. The lack of mixing before this time cannot clearly be linked to meteorology or flow conditions, neither of which showed unusual behavious compared to the rest of the record. The period before 7 August was also marked by inverse stratification of the water column (more dense water overlying less dense water, assuming that temperature controlled density).

3.2.2 Radiation modelling at Place Lake

Modelling incident shortwave radiation at Place Lake gave little improvement on the measured value at PM3 (Figure 3.6a). This was probably because received shortwave radiation varies very little across the lake surface due to the large open nature of the area. The majority of sky view factors for lake grid points varied between 0.85 and 0.89. Furthermore, the PM3 site, which was located on the lower end of Place Glacier, was probably quite representative of the topographic

conditions surrounding a typical grid cell on Place Lake. More distinct variation can be seen between the observed and modelled incident longwave energy flux (Figure 3.6b). The modelled averaged lake values are greater than the observed at the Ridge site during cloudless conditions, which is probably an effect of the additional terrain at the lake that dominates the longwave flux on these days. The modelled averaged values were used in the calculation of the lake heat budget and in the lake temperature modelling.

3.2.3 Lake heat budget

Figure 3.7 shows hourly (in some cases averaged from 10 min data) recorded and calculated heat fluxes over Place Lake, as well as the total heat flux and the heat content of the lake, over the second half of the study period. The heat fluxes are also summarised in Table 3.1. Over the 22 day period shown, Place Lake lost 0.8 MJm^{-2} of energy (this quantity does not account for advective energy associated with precipitation, which was assumed to be minimal compared

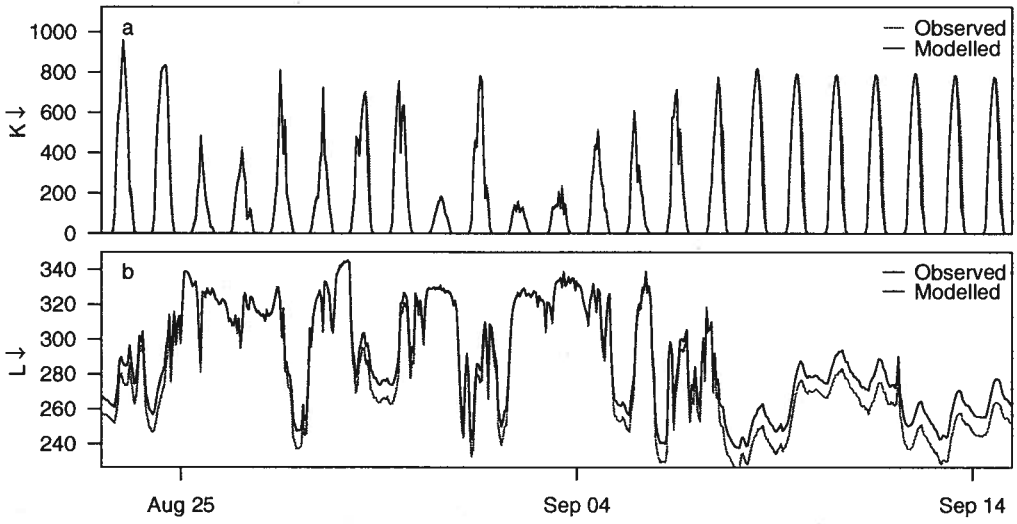

Figure 3.6: Times series of observed (at PM3 and Ridge) and modelled averaged (a) incident shortwave radiation and (b) incident longwave radiation at Place Lake

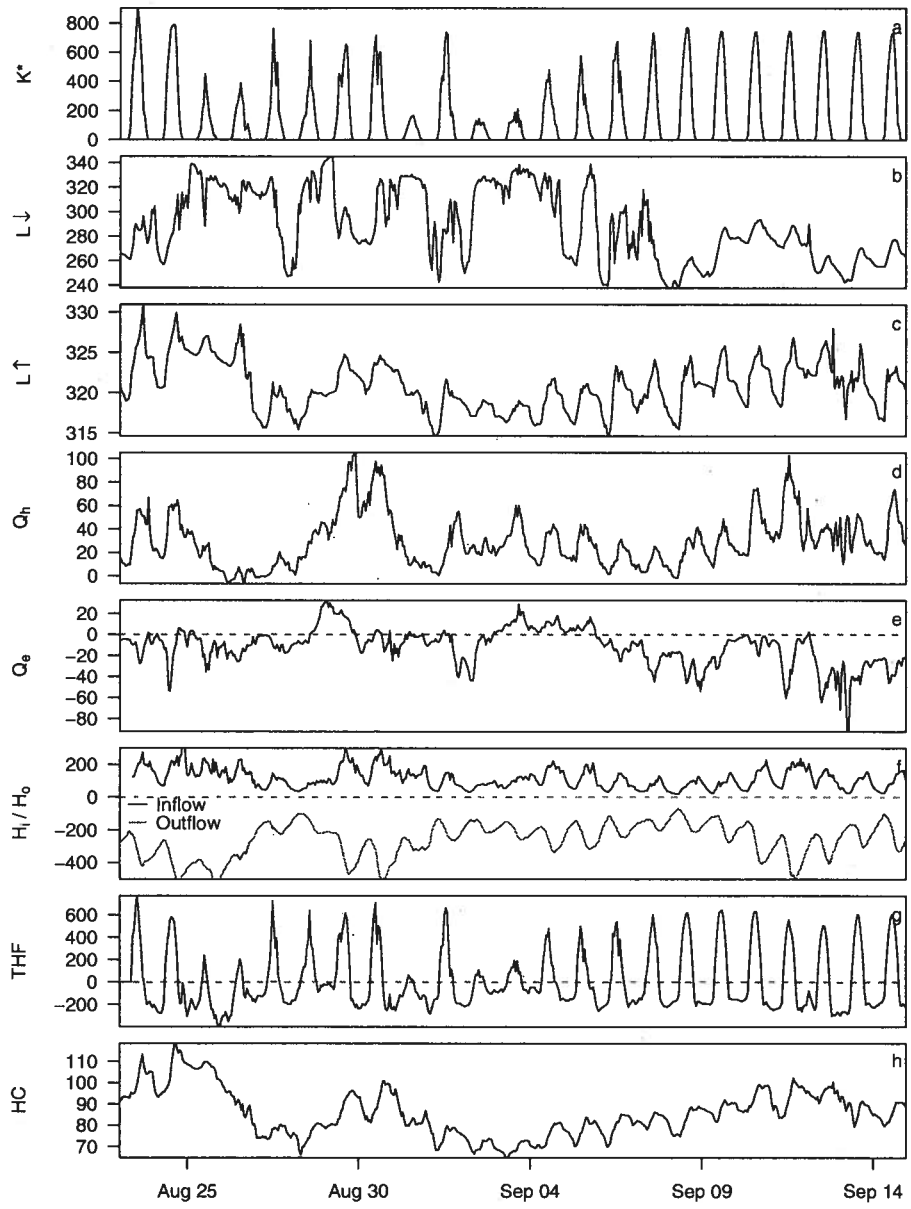

Figure 3.7: Place lake heat fluxes in Wm^{-2}, where (a) is modelled averaged net shortwave radiation, (b) is modelled averaged incident longwave radiation, (c) is emitted longwave radiation, (d) is sensible heat flux, (e) is latent heat flux, (f) is energy associated with the inflow and outflow, and (g) is the total heat flux of Place Lake. (h) shows the heat content of the lake in MJm^{-2}

to the other fluxes). While the measured total heat content of the lake indicated a slightly greater loss of energy, this number shows good agreement with that of the total heat flux. The calculated gain in energy only represented approximately 0.1% of the diurnal amplitude of the total heat flux, and thus was probably at least partly due to measurement error. The biggest source of heat to the lake was absorbed longwave radiation, which was countered by the biggest sink, emitted longwave radiation. Energy gained from absorbed shortwave radiation was for the most part balanced by the net heat exchange of inflows and outflows. The sensible and latent heat fluxes had a relatively insignificant net effect, as did the advective flux associated with evaporation.

The important heat fluxes for determining the heat content of the lake are the inflow and outflow advective fluxes and the absorbed shortwave radiation. A peak in the outflow flux around 28 August appears to have caused a drop in lake heat content at the same time (Figure 3.7). Between 4 and 12 September, a period of increasingly fine weather and consistently high absorbed shortwave flux, the lake heat content rose steadily and was relatively unaffected by

Table 3.1: Total energy added to Place Lake by each heat flux over the 23 day period

Heat Flux	Total (MJm^{-2})
Absorbed (net) shortwave	294.0
Absorbed longwave	550.83
Emitted longwave	-609.7
Latent heat	-22.9
Sensible heat	56.2
Advective: inflow	216.5
Advective: outflow	-486.2
Advective: evap/cond	-0.1
Total	-0.8
ΔHC	-2

fluctuations in the outflow advective flux.

3.2.4 Lake modelling

Modelling the lake as a Continuously Stirred Tank Reactor (CSTR) resulted in minimal temperature change between inflow and outflow water (Figure 3.8). A comparison of Figures 3.8 and 3.4 shows that modelled lake temperatures replicate inflow temperatures.

For the epilimnion model, in which the volume of the lake is effectively reduced to the volume of the epilimnion, lake temperatures were over-predicted by 6 to 10°C (Figure 3.9). Altering the depth of the epilimnion in an attempt to distribute excess energy across a larger volume of water failed to have a considerable effect on the model.

Figure 3.10a shows the results of the initial DYRESM run. Compared to the observed data in part (c), temperatures were over-predicted at the surface and under-predicted at greater depths. There was a relatively good match between the second DYRESM run (in which the inflow entry height was allowed to vary with discharge) and the observed lake temperatures (Figure 3.10), although some over-prediction still occurred in the surface layers. Figure 3.11 compares observed and modelled temperatures at 6 selected depths. Both diurnal and synoptic scale fluctuations match relatively well at all depths. The diurnal amplitude of temperature fluctuations decreases with depth in both the modelled and and the observed records. The more severe surface over-prediction (marked by the dense white band in Figure 3.10, can be seen around 7 August in panels (d), (e) and (f). The best overlays for all depths occurred around 3 September, which corresponds to a period of two consecutive overcast days.

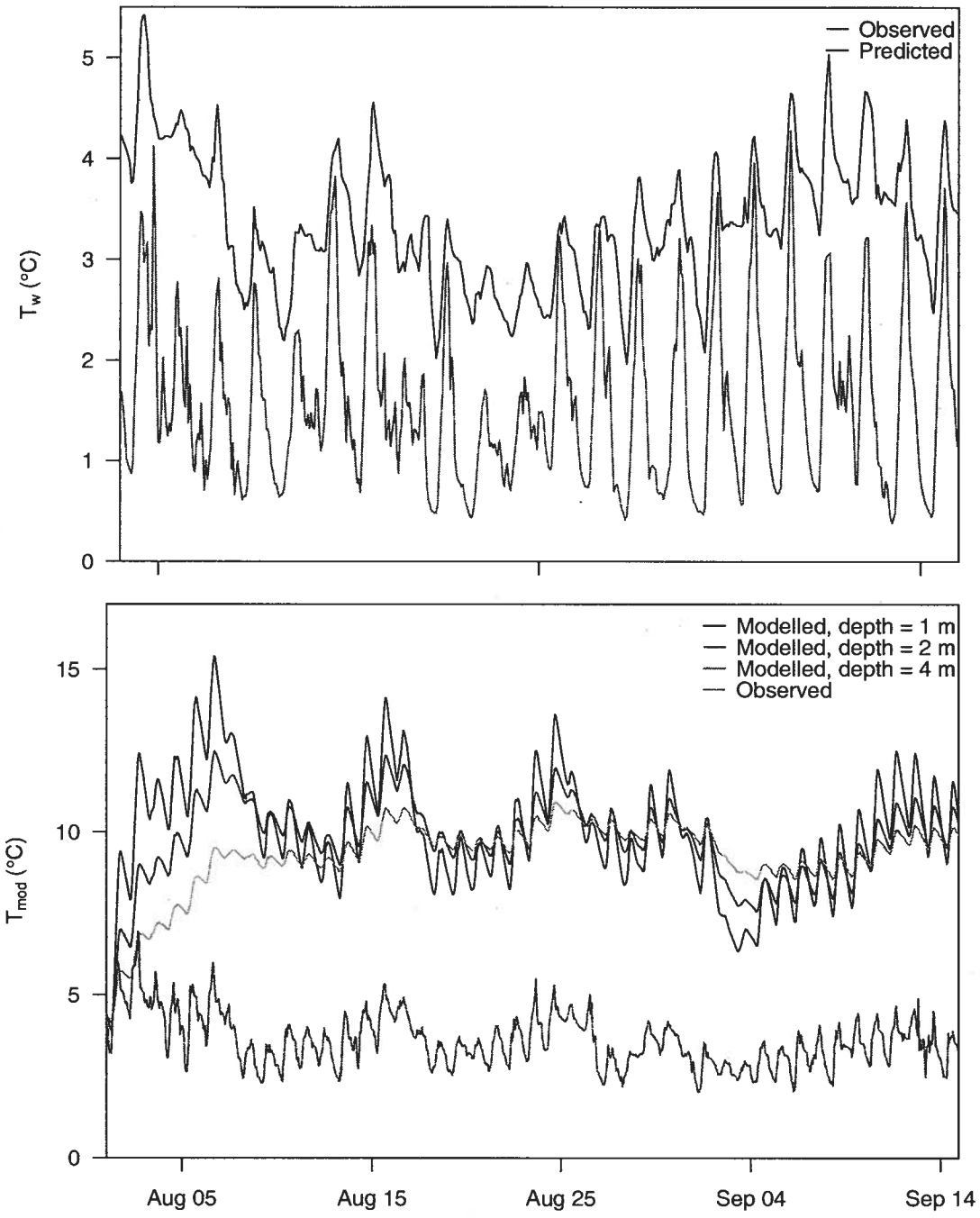

Figure 3.9: Place Lake outflow temperatures, epilimnion model

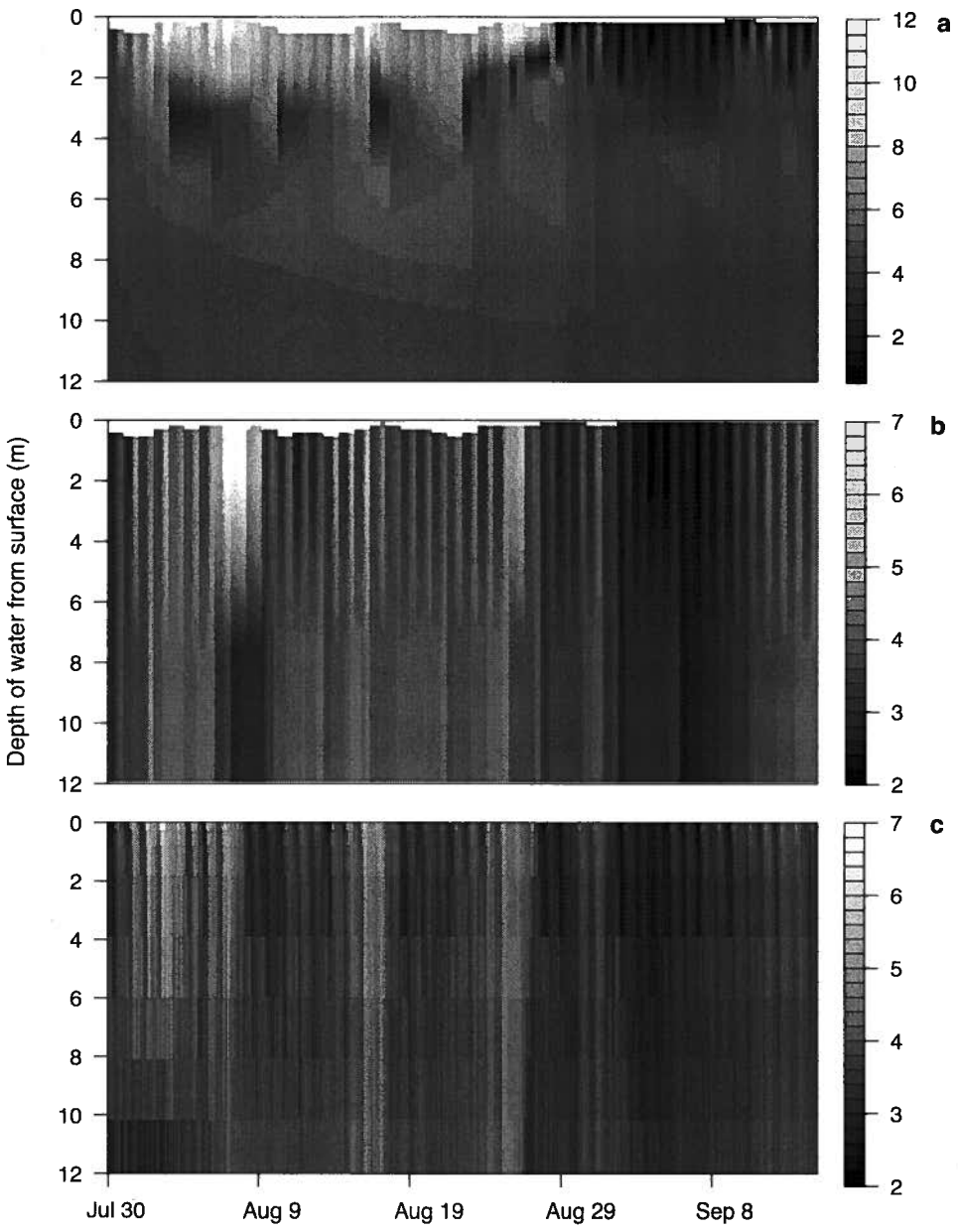

Figure 3.10: Modelled and observed temperature profiles at Place Lake: (a) predicted by DYRESM run 1, (b) predicted by DYRESM run 2 and (c) observed. Note that the modelled surface fluctuates as a function of lake level, but the observed surface does not.

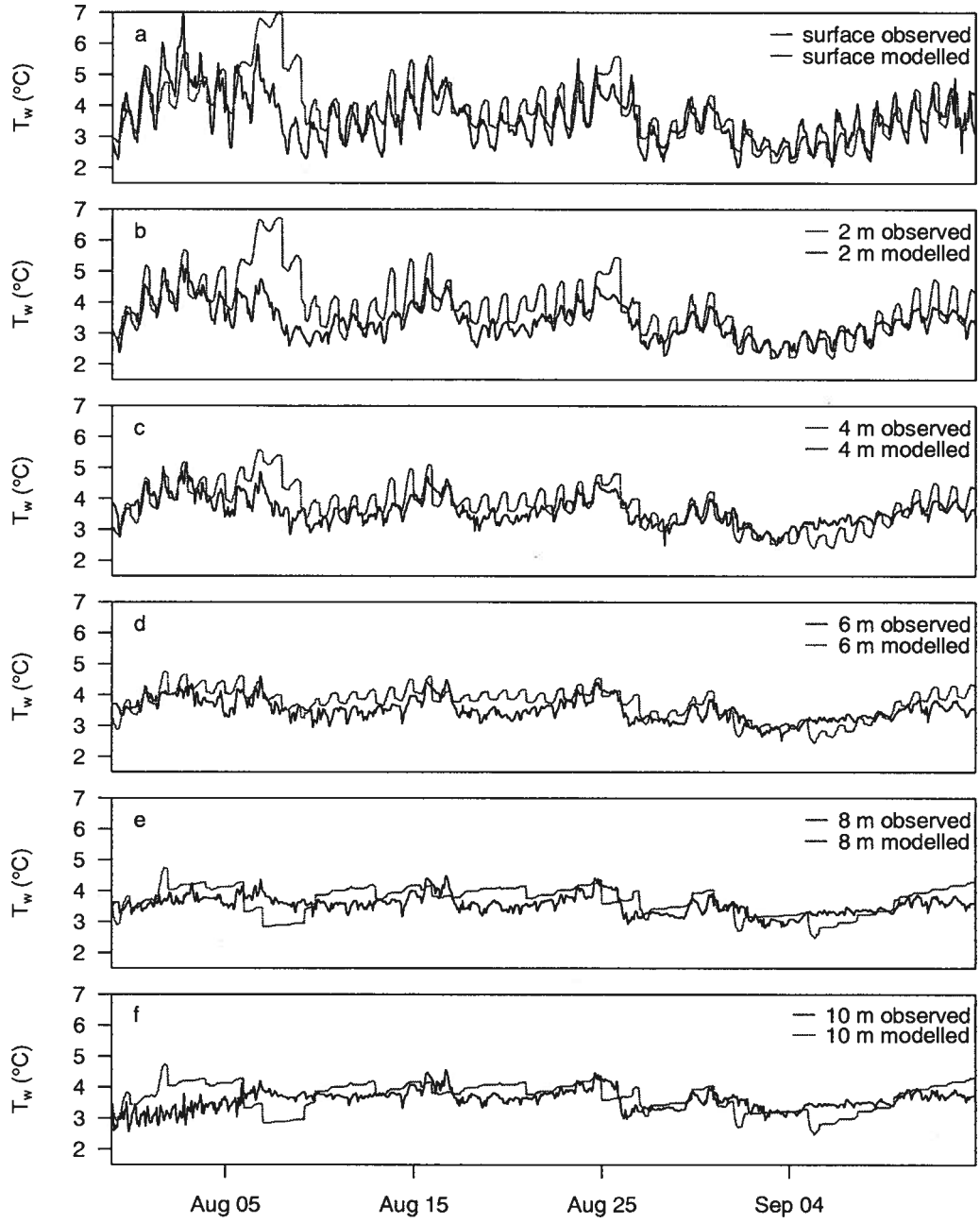

Figure 3.11: Time-series of observed and DYRESM modelled Place Lake temperatures at 6 depths from the surface

3.3 Alpine Reach

3.3.1 Overview

Downstream warming in the alpine study reach occurred throughout the study period. Warming was typically greater during clear sky days and usually remained between 0.5 and 1.5°C. Diurnal fluctuations were greater at PCMS compared to the treeline site.

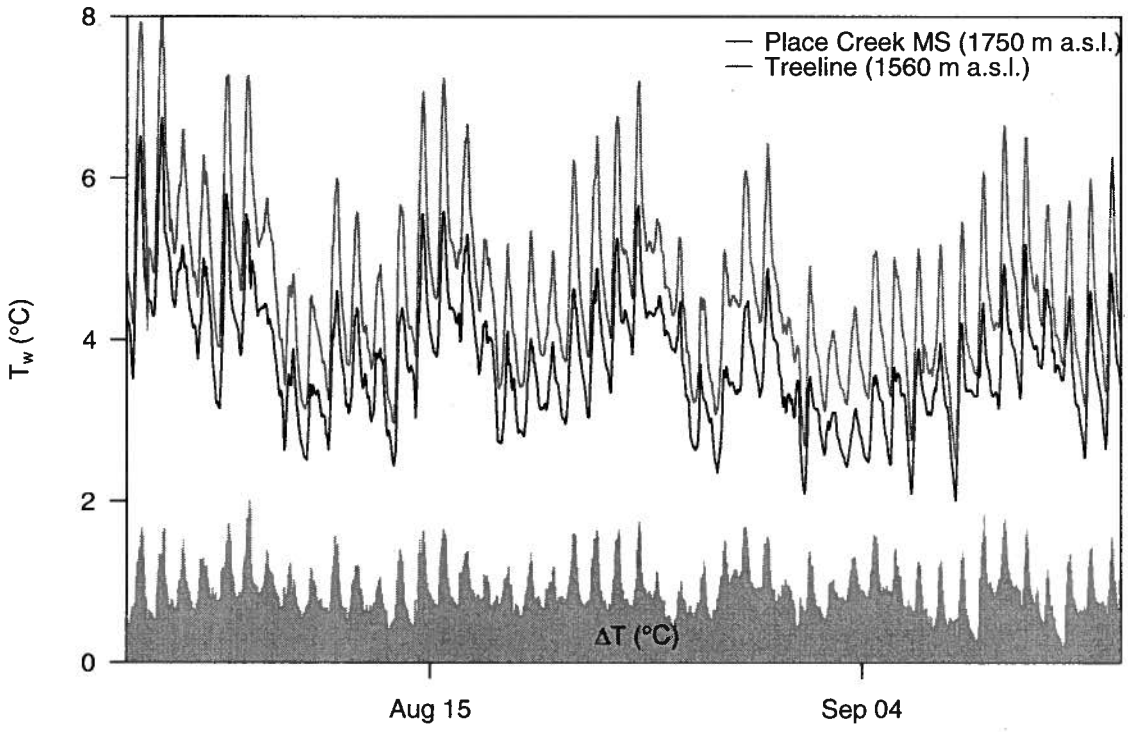

Figure 3.12: Observed stream warming between Place Creek MS and the treeline

3.3.2 Radiation model performance

Parameterising the stream surface albedo as a power function of discharge improved the radiation model (comparison not shown). Figure 3.13 shows that the modelled albedo varied between

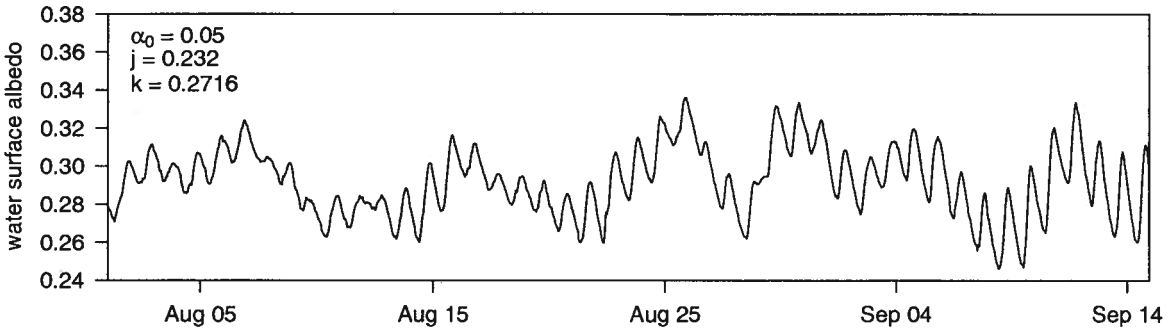

Figure 3.13: Time series of water surface albedo values used in radiation model, parameterised as a power function of discharge

0.25 and 0.34, depending on the magnitude of the flow. Errors associated with the model are discussed in detail in Chapter 4. Figure 3.14a shows general agreement between the trend of observed versus modelled net radiation and the 1:1 line (low mean bias), although a slight curve in the data suggests over-prediction at medium values of net radiation and under-prediction at high values. In Figure 3.14, the data shown in part (a) have a lower RMSE than those in

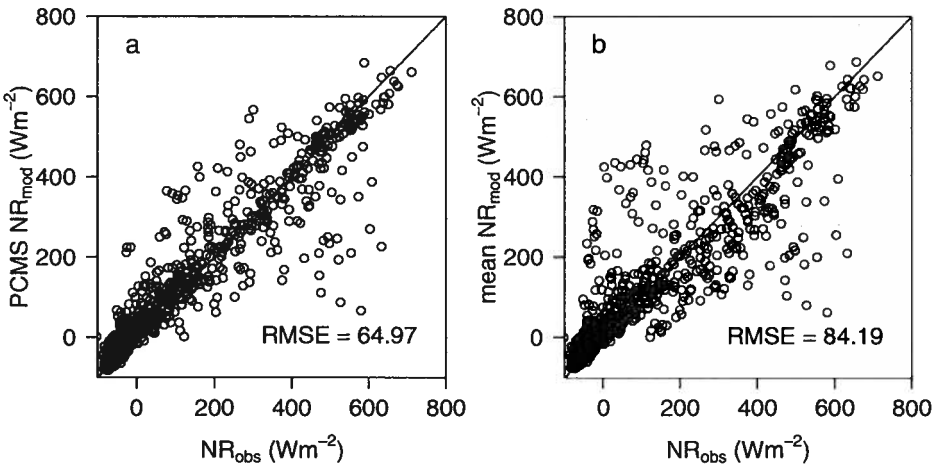

Figure 3.14: Scatter plots of predicted vs. observed net radiation for (a) observed versus modelled data at PCMS, and (b) observed versus reach averaged modelled data

part (b). The reach-averaged net radiation differs sufficiently from the site-specific value to justify the use of a spatially distributed model. Sky view factors varied between 0.62 and 0.86, which suggests that the effects of terrain shading are significant enough to warrant the spatially distributed radiation modelling in this reach.

The radiation model performed best on clear sky days, when the direct component of incident shortwave radiation dominated and passing clouds were minimal (Figure 3.15). However,

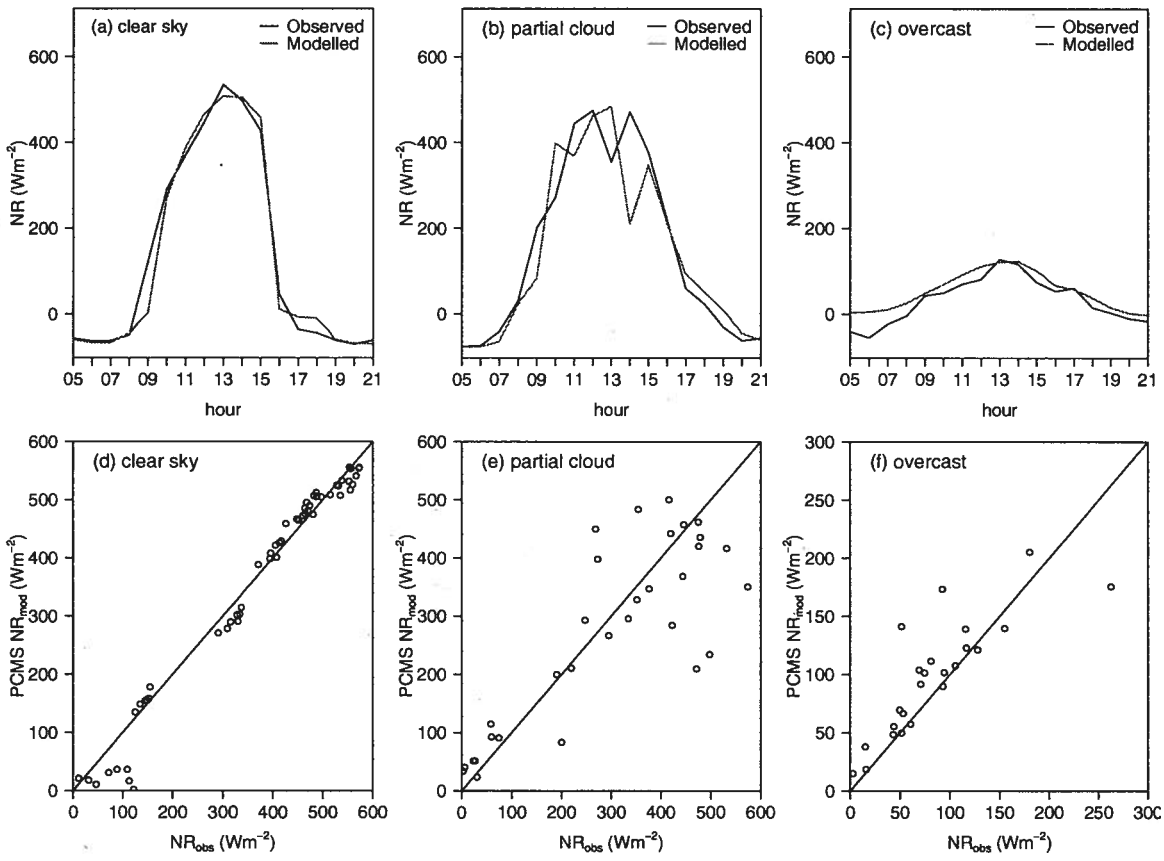

Figure 3.15: Time series of predicted and observed net radiation at PCMS for (a) a selected clear day, (b) a partially cloudy day and (c) an overcast day. (d), (e) and (f) show scatter plots of observed vs. modelled net radiation at the same site for selected days with similar cloud conditions to (a), (b) and (c), respectively

all clear days did feature minor under-prediction at the peak of net radiation and over-prediction during the late afternoon. Figure 3.15b compares the observed and modelled net radiation for a partially cloudy day. The mismatch in the timing of daytime variability demonstrates the effect of partial cloud cover, which tended to shade PM3 and PCMS at different times, resulting in amplified scatter of the errors (Figure 3.15 e). Slight over-prediction can also be seen in the late afternoon. Over-prediction on overcast days was likely a result of errors inherent to the equations used to calculate longwave radiation and the diffuse component of incident shortwave radiation. Under all sky conditions, there was a good match in the onset of the diurnal rising limbs and the termination of the falling limbs,which suggests that the shortwave terrain mask adequately represented the timing of the sunrise and sunset.

3.3.3 Stream heat budget modelling results

Model 1 performed poorly when applied using both the observed and reach averaged modelled net radiation (Figure 3.16a and e). In each case, the scatterplot of observed and modelled data shows a high mean bias (departure from the 1:1 line). Visual inspection shows that Models 2, 3 and 4 all produced a better fit between observed and predicted data than Model 1. Table 3.2 provides goodness-of-fit statistics for each version of the three hybrid models. When either the observed or the modelled net radiation was used (variants a or b), all of the five test statistics indicated a better fit when moving from Model 2 to Model 3 to Model 4. Furthermore, model performance improved when modelled net radiation was introduced in all of Models 2, 3 and 4. Model 4b was the best model.

Parameter estimates for the four constants are shown in Table 3.2. The two constants associated with the substituted width term (a and b) were both reduced by approximately 20 to 30 % between Models 2 and 3. The constant a increased when the modelled net radiation was used in all models (variant b of each model), whereas b remained relatively unchanged. The constant c increased by approximately 50% between Models 3 and 4, but decreased between

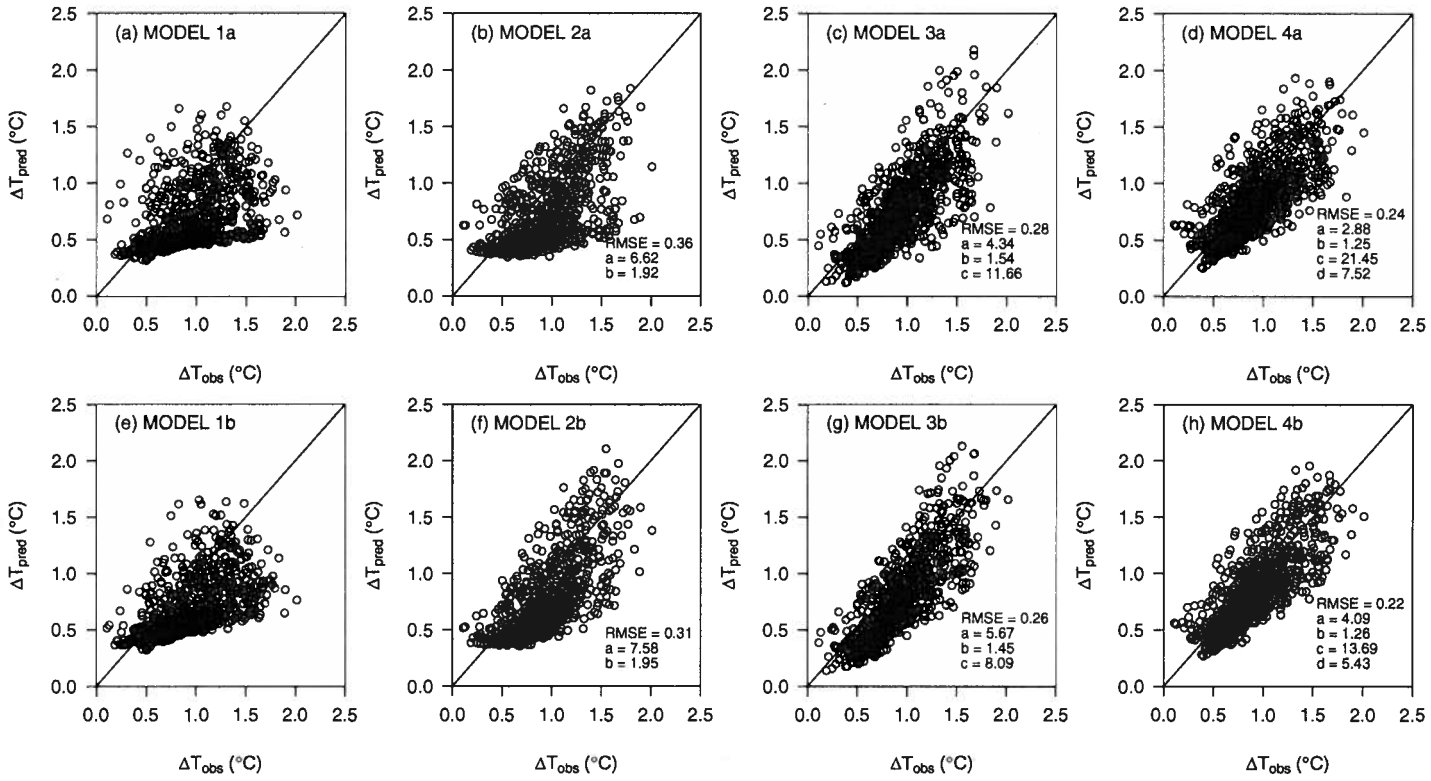

Figure 3.16: Observed versus predicted stream warming between Place Creek MS and the treeline for the four models, each with two variants.

Table 3.2: Results of NLS analysis for two variants of Models 2 and 3 showing parameter estimates (p-value shown in parentheses), RMSE, MAE, MBE, AIC and I^2 (pseudo R^2)

Model	*a*	*b*	*c*	*d*	RMSE (°C)	MAE (°C)	MBE (°C)	AIC	I^2
2a	6.62	1.92			0.355	0.299	0.241	835.510	-0.341
3a	4.336	1.537	11.655		0.285	0.240	0.181	360.384	0.138
4a	2.878	1.248	21.448	7.523	0.239	0.192	0.087	-19.936	0.395
2b	7.579	1.946			0.301	0.263	0.196	513.222	0.005
3b	5.666	1.452	8.086		0.256	0.218	0.159	127.093	0.306
4b	4.094	1.257	13.692	5.429	0.222	0.180	0.085	-178.008	0.478

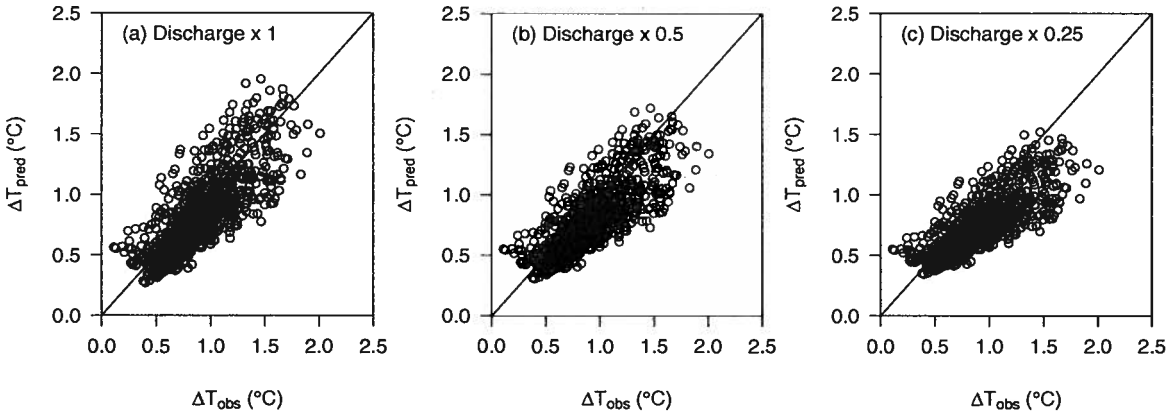

Figure 3.17: Scatterplots of predictions from model 4b against observed downstream warming for (a) measured discharge, (b) half the measured discharge and (c) one-quarter the measured discharge

model variants a and b. In each of Models 2, 3 and 4, the substituted width term was positively correlated with discharge and had a positive effect on overall stream warming. This effect is

demonstrated in Figure 3.17, which shows the results for Model 4b for reduced discharge, in order to explore the effect of reduced flows on stream warming. Under scenarios of both halved and quartered stream discharge, less stream warming occurred throughout the alpine reach.

Figure 3.18 shows the surface heat fluxes as measured or calculated before modification in the modelling process. Unsurprisingly, the dominant flux is net shortwave radiation. Given that absorbed and emitted longwave radiation generally cancel each other out, the next most important heat flux appears to be sensible heat exchange across the water surface. If enhanced by a factor of 13 (as in Model 4b), this flux would periodically exceed that of net shortwave radiation.

Figure 3.19 shows the errors associated with Models 2b, 3b and 4b plotted over time and by hour. The model 4 errors over time are more evenly spread above and below the zero line than those for Models 2 and 3. When plotted by hour, there is a clear trend whereby the model over-predicts in the late morning and under-predicts in the mid-afternoon.

Figure 3.20a shows a time series of observed and modelled stream warming between PCMS and the treeline using Model 4b with the reach-averaged modelled net radiation. Part (b) shows a time series of associated errors. Examination of part (a) shows that the errors are relatively consistent throughout the study period. Part (b) shows that the same errors do not show any noticeable trend over time.

In summary, Model 4b exhibits the best fit between observed and modelled data. The errors for this model, however, show some correlation with time of day, but no continuous correlation over time. The magnitude of the coefficients in Model 4b provide some interesting insights into the processes that control stream temperatures in the alpine reach, which will be discussed in the next chapter.

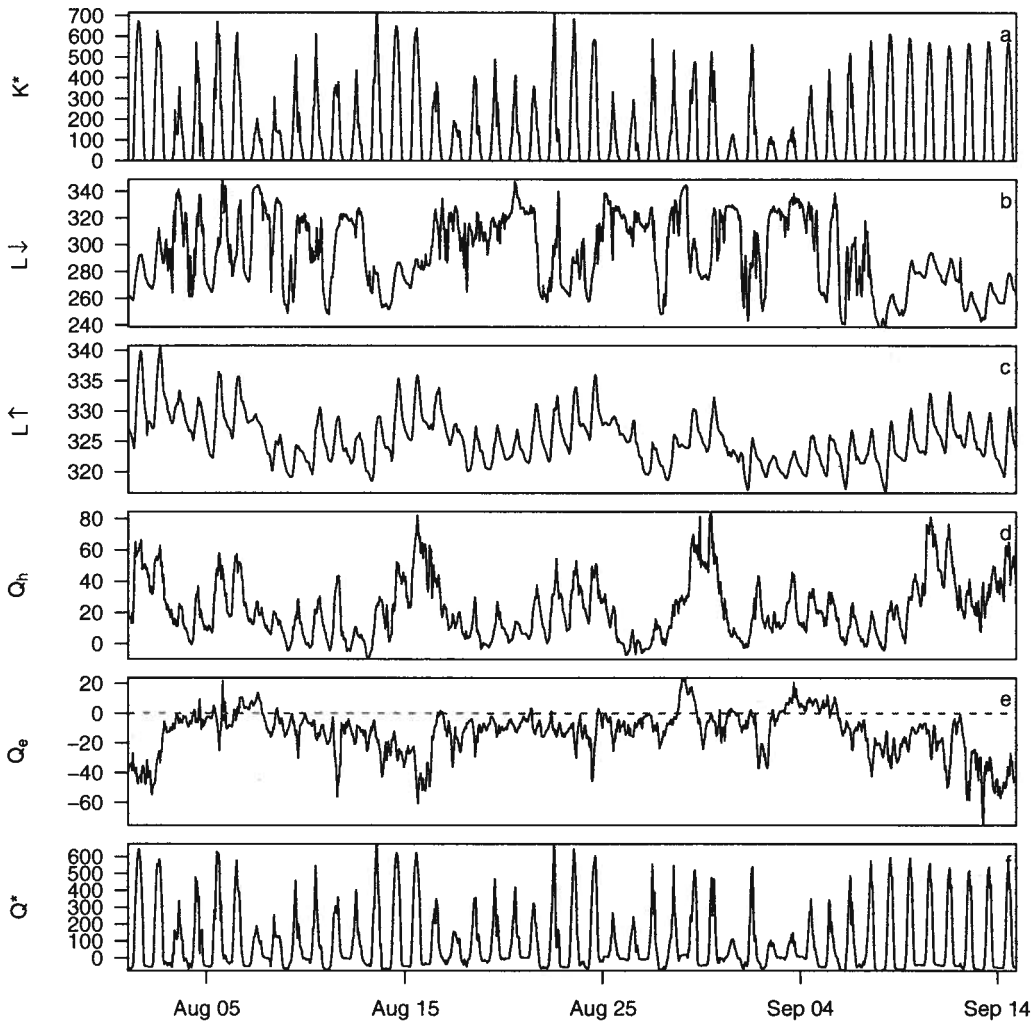

Figure 3.18: Measured and calculated heat fluxes in Wm^{-2} for the alpine reach: (a) net shortwave radiation, (b) incident longwave radiation, (c) emitted longwave radiation, (d) sensible heat flux, (e) latent heat flux, (f) modelled net radiation

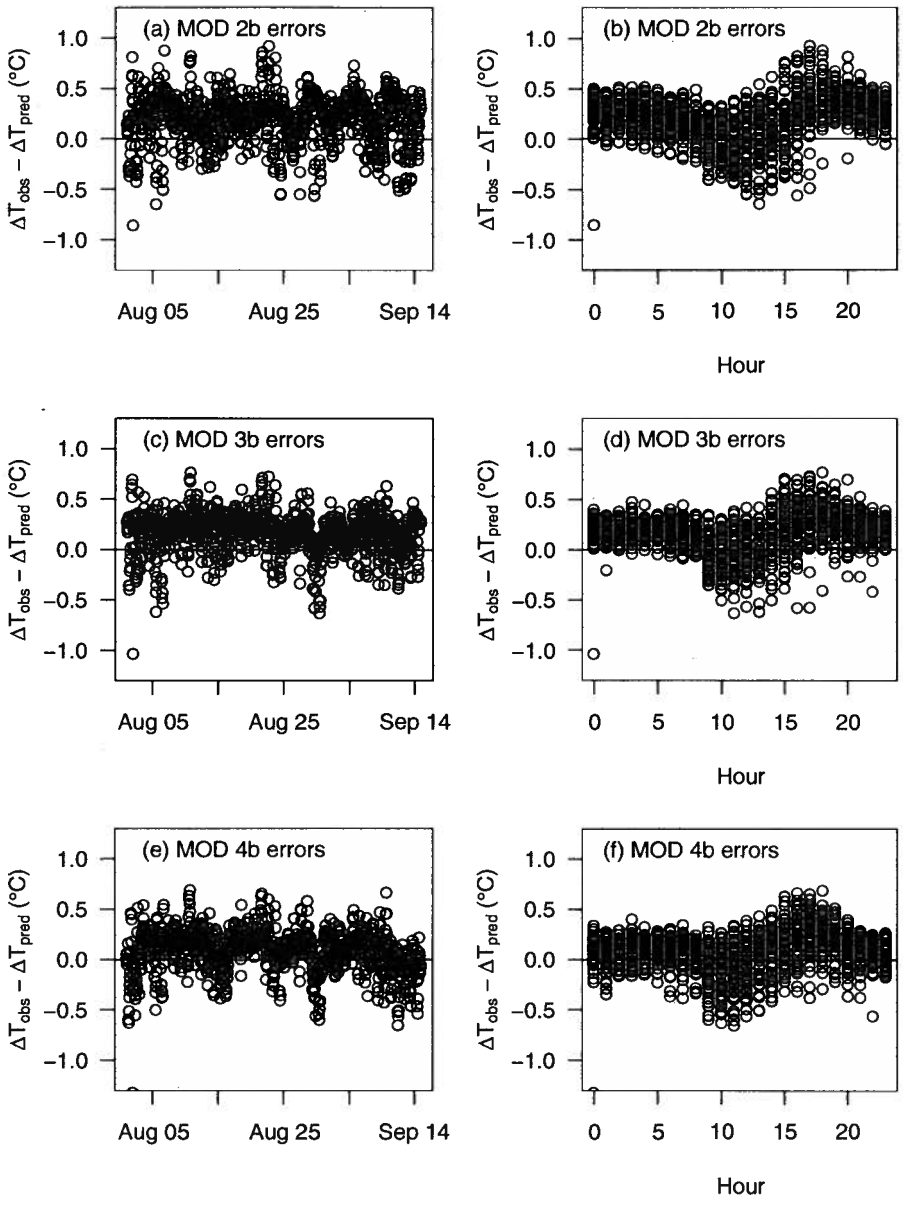

Figure 3.19: Errors associated with Models 2b, 3b and 4b plotted over time and by hour

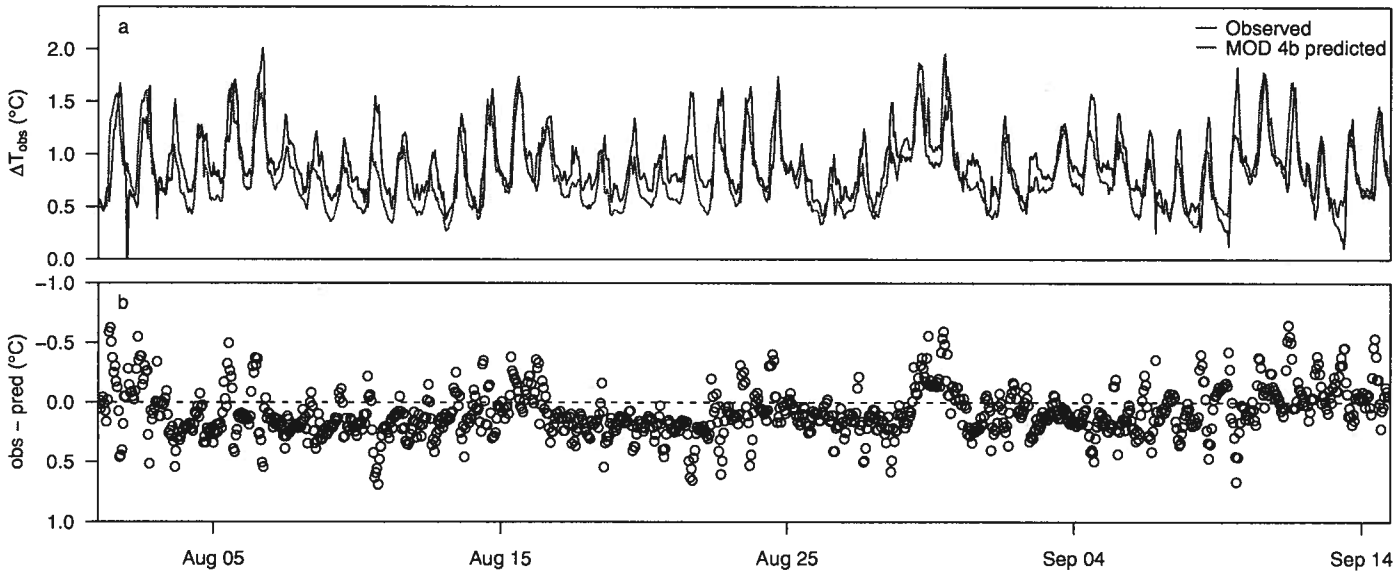

Figure 3.20: (a) time series of observed and modelled stream warming for Model 3 using the reach averaged modelled net radiation, (b) associated errors for the same model

Chapter 4

Discussion

This discussion is organised into three sections: (1) a comparison of applied models used in the Place Lake analysis, discussion of the controls on lake stability and mixing, and suggestion of the overall controls on outflow temperatures; (2) modelling net radiation in the alpine reach, interpretation of the stream heat budget models, and a discussion of observed warming rates in the context of previous work; (3) a synthesis of the findings from (1) and (2) and their implications for the effect of glacier retreat on stream temperature.

4.1 Place Lake

4.1.1 Effect on stream temperature

Assuming that water discharging from the glacier was at 0°C, Place Lake inflow temperatures were controlled by energy exchanges occurring in the upper lake and a short length of connecting stream, the net effect of which was up to 4°C of warming. The shallow depth of the upper lake was probably responsible for most of this warming. On average, Place Lake had a warming effect of 1.8°C on inflowing water. Both Weirich (1986) and Uehlinger et al. (2003) observed similar warming in high altitude proglacial lakes, both of which were, however, significantly larger than Place Lake (see Table 4.1 for a comparison). To an extent, therefore, it seems that warming in proglacial lakes is controlled by characteristics other than the volume and surface area of the lake (such as number and volume of inflow channels, lake bathymetry and prevailing meteorological conditions). Within-lake thermal heterogeneity has also been reported between lakes in similar glacio-climatological settings (Warren and Kirkbride, 1998), so it is reasonable

Table 4.1: Comparison of alpine lake studies

	Place Lake	Weirich (1986)	Uehlinger et al. (2003)	Robinson and Matthaei (2007)
location	Coast Mtns, BC, Can.	Purcell Mtns, BC, Can.	Bernina Massif, Swiss Alps	Macun, Swiss Alps
water inputs	GM SM	GM SM	GF SM	GW SM
surface area	0.07 km^2	0.24 km^2	0.22 km^2	0.12 km^2
volume	432,000 m^3	1,190,000 m^3	1,500,000 m^3	nd
elevation (a.s.l.)	1830 m	2195 m	2159 m	2631 m
residence time	*4 days	9-13 days	2-3 days	nd
****warming**	1.8°C	$^{+}$1.6/1.9°C	2-4°C	6-8°C
notes	period mean	period mean	approx. range	approx. range

* assumes mean depth of 6 m and complete mixing of water column
** 1977/1978 summer mean
nd = no data
GM = glacier ice-melt
SM = snow-melt
GW = groundwater

that outflow temperatures may also vary widely between similar lakes. In Switzerland, Robinson and Matthaei (2007) observed warming of up to 8°C in a high elevation non-glacier-fed lake of comparable size to Place Lake, which suggests that much more warming occurs without the influence of glacier ice-melt.

The consistently close correspondence between mid-lake surface and outflow temperatures suggests that Place Lake experienced little surface lateral thermal variability, at least between the mid-lake measurement site and the outflow. This similarity also suggests that cycles of mixing and stratification were uniform across the lake, and that it wasn't the case that water warmed up as it approached the outflow. Mid-lake and outflow temperatures were affected more by diurnal temperature fluctuations than deeper water, resulting in greater heat loss via

the outflow during the day than the night. These fluctuations suggest that upper layers were subject to greater heating via surface exchanges, and possibly that the water column was not completely mixed at all times.

4.1.2 Lake heat budget

The heat budget of Place Lake revealed that the most important source of energy (in terms of being responsible for fluctuations in total heat content) came from the net shortwave flux and the most important sink was heat loss via the outflow channel. The close match of the integrated heat fluxes with the observed total heat content of the lake reinforces the validity of this finding. This match also confirms that no thermally significant heat fluxes were omitted from the calculated total heat flux, and that the assumption of minimal groundwater discharge was reasonable. This dominant advective control on lake heat content is uncharacteristic of most temperate water bodies (Wetzel, 1975), but has been commonly observed in small proglacial lakes (although not shown through a heat budget analysis) (Gilbert and Shaw, 1981; Weirich, 1986). Most researchers studying lake heat budgets have identified surface fluxes as dominantly controlling heat content (Gibson and Stewart, 1973; Frempong, 1983; Schertzer, 1978).

4.1.3 Lake temperature modelling and controls on lake stability

The CSTR model was based on the assumption that the lake is well-mixed, as was found to be the case by Weirich (1986) for a small proglacial lake. The CSTR model, however, failed to replicate surface temperatures based on advective and surface energy exchanges. Distributing the entire heat content of the lake evenly throughout the water column resulted in outflow temperatures that were much lower than those observed. From one perspective, the failure of the CSTR model is not surprising given (1) the irregular shape of Place Lake, which might prohibit mixing, and (2) the complex nature of observed cycles of mixing and stability. In temperate lakes, and many alpine lakes, it is often the case that summer surface heating increases the

thermal resistance to mixing as surface temperatures rise above the temperature of maximum density, thus preventing complete circulation of the water column (Wetzel, 1975). This effect is exacerbated by a lack of wind. Loss of stratification may occur if surface waters cool, and sink by a combination of convection currents and wind induced circulation. However, the effect of summer surface heating in proglacial lakes (and thus resistance to mixing) is moderated by cold inputs of snow- and ice-melt. The density of cold inflows is further increased by dissolved and suspended sediment from glacial erosion, which causes inflows to plunge to the lake bed and induce mixing. Since Place Lake temperatures all fluctuated around 4°C (with some exceptions), thus producing minor temperature-induced density differences, mixing was probably controlled more by the effect of sediment load on density and wind induced surface circulation. Weirich (1986) observed similar sediment forced underflows in Expectation Lake, together with a lack of thermal control on density. Expectation Lake lies in a similar glacio-geomorphological setting to Place Lake, and features a single inflow and outflow channel. One might expect that mixing only occurs when inflows (and accompanying suspended load) exceed a threshold. While Weirich rarely observed stratified conditions, Place Lake may straddle this threshold throughout the summer, thus explaining the occurrence of cycles of mixing and stability on timescales that match variability in snow and ice melt.

The epilimnion model was based on the hypothesis that inflowing water plunges to the bottom of the lake. In such a case, if there was little mixing between the epilimnion and deeper waters, the effect of inflowing water could be ignored and lake outlet temperature would be controlled by surface energy exchanges. Under conditions of low sediment input to a small glacial lake, Smith et al. (1982) observed the common occurrence of overflows and distinct stratification, which occur when the density of incoming water is less than that of the lake density. When isothermal conditions were observed, yet sediment inputs remained low, homopycnal flow was cited as the dominant cause of mixing. Similarity between outflow and mid-lake surface

temperatures in this study suggested that overflows may be a common occurrence. It was assumed, therefore, that the net advective effect of the inflows and outflows was minimal, and that the temperature of the epilimnion would be uniform both horizontally and vertically across the lake. The severe model over-prediction that was seen was likely due to the fact that some of the energy gained from surface heating during the day was actually being transferred to deeper water (this is unaccounted for in the model), or that underflows or homopycnal flows were driving vertical mixing of the water column.

The CSTR and epilimnion models represented two extreme scenarios, the former being complete mixing at all times and the latter a state of continual stratification. The temperature-depth profiles showed complex cycles of mixing and stratification superimposed on different timescales. The times of mixing played an important role in distributing heat to lower depths (hence over-prediction in the epilimnion model), whereas intermittent stratification meant that the surface water was often significantly warmer than the water below (hence under-prediction in the CSTR model).

The advantage of DYRESM was its ability to model vertical heat exchange within the water column and thus estimate outflow temperatures over time, which was the real limitation of the CSTR and epilimnion models. The initial run of DYRESM gave similar results to the epilimnion heat budget model. Surface temperatures were over-predicted and not enough heat was being distributed to depths below the epilimnion (note that DYRESM did not include a function that determined lake mixing). The second run accounted somewhat for the sediment load of the inflow stream by applying a discharge dependent threshold to control the entry height of the inflow. This effect induced mixing within the lake model that represented the observed temperature profile over time. The success of the DYRESM model is encouraging given that density is not the only physical parameter that controls the fate of inflowing water; it is also a function of the shape of the inflow channel and the rate of flow, as demonstrated by Mathews

(1956). These results reinforce the hypothesis that during the summer, Place Lake straddles a discharge dependent threshold that controls mixing and stability, and that underflows, overflows and homopycnal flow are all common occurrences. Indeed, the time series of lake temperatures at selected depths showed superimposed cycles of mixing and stratification that took place on different time scales that were likely driven by different processes.

4.1.4 Physical controls on outflow temperatures

Outflow temperatures were controlled by (1) the total heat content of the lake and (2) cycles of mixing and stratification within the lake. The total heat content showed diurnal fluctuations that corresponded with the total surface heat flux, although there was a lag present. Longer term fluctuations were also correlated with the dominant surface energy exchange, incident shortwave radiation. It was the advective terms, however, which consistently regulated the heat content of the lake.

The magnitude and sediment content of the inflows were a dominant control on lake mixing, producing periodic cycles of underflows, much like those observed by Weirich (1986), which resulted in short-lived cycles of mixing and stratification. Overflows may have occurred during times of lower inflow sediment content. It appears that the density of the inflow to Place Lake tended to fluctuate above and below a threshold that is necessary to induce mixing via underflows. Currently, the warming effect of Place Lake is moderate, possibly because the water column appears to be mixed approximately 50% of the time during the late summer, which arguably has an overall cooling effect on outflow temperatures. The estimated low residence time of 4 days at Place Lake is an alternative explanation for the observed moderate warming.

Unlike most freshwater lakes, therefore, both stability and the heat content of small alpine glacier fed lakes are strongly influenced by inflows and outflows. Surface energy exchanges, therefore, play a subordinate role given (1) the consistently low temperature of the inflows (and the fact the surface exchanges can do little to mediate this), and (2) the fact that changes in

surface temperatures associated with surface heating result in relatively small changes in water density.

4.2 Alpine reach

No significant attempt has previously been made to apply a predictive energy budget model to an alpine proglacial stream (to the knowledge of the author). Extensive literature exists, however, on energy budget applications to lower gradient streams. Process-related heterogeneity, due to steep terrain, cascading flow and varying stream discharge, presents new challenges for stream energy budget modelling. Capturing the magnitude of the dominant energy exchanges either requires extensive field measurement (which is rarely a practical possibility), or spatially distributed modelling.

4.2.1 Modelling net radiation in an alpine stream

Attempts to account for the spatial variability of shade in stream heat budget models have typically involved a consideration of the effects of topography and canopy cover (Rutherford et al., 1997; Moore et al., 2005a; Guenther, 2007). While canopy cover is minimal in the alpine environment, a consideration of topographic shading, slope and aspect is crucial. All four stream heat budget models in this study displayed a better fit when the reach-averaged modelled net radiation was used.

Modelling the spatial variability in solar radiation in the alpine reach of Place Creek provided new insights into the importance of the role of steep topography on stream warming in alpine channels. Parameterising the water surface albedo as a power function of discharge significantly improved the radiation model. These results imply that cascading stream reaches have particularly high albedos that vary significantly over time due to changes in stream flow. The positive correlation between albedo and discharge was likely a function of the increased cascading nature of the water at higher flows (causing increased frothiness). While the mag-

nitude and variability of stream surface albedo is probably not unique to alpine streams, it is a crucial process consideration in such reaches due to the intense insolation caused by the lack of shade and high elevation. Steep topography also alters the angle of incidence of direct beam shortwave radiation, which in turn alters the sky view factors and the amount of diffuse shortwave and incident longwave radiation that reaches the stream surface. In this study, the range of sky view factors increased from 7 to 24 % when the angle of solar incidence was corrected for the slope of the channel. While the effects of slope and aspect are important in any steep stream, in alpine catchments much of the incident longwave radiation comes from the topography, as opposed to riparian vegetation, and the channel is more exposed to both direct beam and diffuse shortwave radiation.

4.2.2 Alpine stream heat budget modelling

The failure of Model 1 to replicate observed downstream warming in the alpine reach of Place Creek reinforces the hypothesis that alpine proglacial stream temperatures are controlled by a different set of dominant processes to those in lower-gradient streams. As expected, the improved fit of Model 2 implied that the channel width was better represented by a power function of discharge than a static number. The coefficients in models 2, 3 and 4 suggested a positive correlation between discharge and stream warming. This finding is somewhat surprising given that past researchers have identified inverse correlations between stream temperature and discharge in a variety of catchments and at differing timescales (Hockey et al., 1982; Gu et al., 1998; Webb et al., 2003). Most of these studies, however, were based on empirical correlations between air temperature, stream temperature and discharge as opposed to process-based information. At Place Creek, it seems reasonable that as the channel becomes wider at higher flows more stream surface is exposed to the atmosphere, thus causing more warming to occur. An additional warming effect could be cause by diurnal variations in stream width and associated enhanced warming via the stream bed, whereby unsubmerged boulders could

warm substantially in the afternoon, then transfer this heat to the water as flows rise and the boulders become submerged. Accounting for both spatial and temporal channel width variability is particularly important in proglacial streams due to the variable nature of stream discharge.

Results from both Models 3 and 4 suggest that the sensible and latent heat fluxes were underestimated using equations developed from observations in low-gradient streams. There are a number of possible explanations for the heightened importance of these turbulent fluxes. The cascading nature of the flow in steep proglacial channels may have enhanced the downward flux of sensible heat by effectively increasing the stream surface exposure to the atmosphere. Latent heat transfer could also have been increased by cascading flow, due to enhanced evaporative heat loss as water droplets became suspended in the air or splashed onto boulders. Both of these effects could have been exacerbated by strong winds experienced at high elevation.

In Model 4b the sensible heat was raised by a factor of 13.69, implying that its net effect was at times greater than that of the net shortwave radiation. It is feasible, therefore, that the coefficients c and d also accounted for the effects of processes that were not included in the model. Above-treeline reaches could be particularly susceptible to warming via the stream bed as the ground heats up due to exposure to direct solar insolation. This effect would be exacerbated by diurnal fluctuations in stream width and depth which caused water periodically to come into contact with warm boulders on the edge of the channel. The cascading nature of the flow might also have caused water to splash onto rocks, heat up and subsequently re-enter the channel.

The errors associated with Models 2, 3 and 4 all displayed systematic diurnal patterns. Under-prediction during the late afternoon may have been caused by over-estimation of the emitted longwave flux, and vice versa for the over-prediction during the late morning. Emitted longwave radiation was a calculated term that was not adjusted in the hybrid models, the

equations for which may not apply to the alpine environment. Alternatively, the energy transfer via the stream bed may have contributed more heat during the late afternoon than in the morning. While the final model coefficients represented averaged conditions over the course of the study period, their true values were probably variable over time. Such variation throughout the course of the day may explain the observed wave-like pattern in the errors.

4.2.3 Warming rates

The rate of stream warming observed in the alpine reach of Place Creek was almost twice that observed by Cadbury et al. (2008) in a below-treeline reach of a New Zealand proglacial stream (1.1°C km^{-1} compared to 0.6°C km^{-1}) (see Table 4.2). Greater warming at Place Creek can be attributed to (1) the lack of stream shading, (2) the intensity of solar radiation at higher elevation (all sampling sites in Cadbury et al. (2008) were below 800 m a.s.l.), and (3) the steeper channel gradient (greater loss of potential energy and frictional warming). Uehlinger et al. (2003) found a similar rate of warming to Cadbury et al. (2008), but in a different environment, located in the Swiss Alps. Measurements were made on a flat glacial floodplain (gradient $< 2\%$) with multiple lateral inflows from a variety of sources. In this case, warming can be attributed to surface energy exchanges (above-treeline) and the effects of varied source water contributions. Note that stream temperature variations among different channels within the floodplain were higher than along the entire main channel (not just in the floodplain). Thermal heterogeneity was linked to pulses of glacier melt. Brown et al. (2005) observed warming rates of 7°C km^{-1} in a steep proglacial channel in the French Pyrenees. Catchment glacier cover, however, was less than 5% and a significant proportion of the downstream flow originated from groundwater sources (discharge was only 0.07 m^3s^{-1} 1 km downstream of the glacier). The reported warming occurred between the snout of one glacier (there were two within the catchment) and a measurement site 1 km downstream, at which point the stream water was composed of water from a variety of origins. Frictional warming would only

Table 4.2: Comparison of alpine stream temperature studies

	Place Creek	Cadbury et al. (2008)	Uehlinger et al. (2003)	Brown et al. (2005)
location	Coast Mtns, BC, Can.	Rob Roy Glacier, New Zealand	Bernina Massif, Swiss Alps	Pyrenees, France
site description	AT PG PL	BT PG	AT PG PL	AT PG
glacier cover	26%	30%	30%	< 5%
water sources	GI SP R	GI SP R	GI SP R	GI SP R GW^{+}
elevation (m a.s.l)	1563 - 1780	400 - 800	2064 - 1998	1850 - 2550
channel gradient	25%	12%	< 2%	70%
observed warming during melt season	1.1°C km^{-1}	0.6°C km^{-1}	0.6°C km^{-1}	7°C km^{-1}
discharge*	1.2 m^{3}s^{-1}	4 m^{3}s^{-1}	2.8 m^{3}s^{-1}	0.07 m^{3}s^{-1}

*mean for period of study period, measured at different locations along main channel
$^{+}$extensive karst groundwater and hillslope aquifers

AT = above treeline
BT = below treeline
PG = proglacial channel
PL = proglacial lake
GI = glacier ice
SP = snowpack
R = rain
GW = groundwater

account for approximately 1.6°C of the observed warming. Stream warming could have been promoted by cascading flow in such a steep channel, the gradient of which was approximately 70%. Unreported data from below the treeline at Place Creek showed a 2.5°C rise in stream temperature over a 300 m elevation drop in a cascading reach, which is much greater than the heat gain due to the loss of potential energy.

4.3 Implications for glacier retreat

4.3.1 Shifts in lake stability

Prolonged glacier retreat will result in reduced streamflow at Place Creek (Collins, 1987; Hock et al., 2005). Two additional consequences are (1) lengthening of the stream channel between the glacier snout and the inflow of Place Lake, resulting in higher inflow temperatures, and (2) reduced inflow sediment load. Given that the density of water in Place Lake is primarily controlled by temperature and suspended sediment concentration, cycles of mixing and stability will be altered with deglaciation. Underflows, which arguably promote mixing of the water column, will become an increasingly rare occurrence (the threshold applied to DYRESM would no longer be exceeded). More persistent stratification, together with less dense inflow water (due to both temperature increase and sediment loss in the upstream channel), could mean that summer inflows merely displace warm surface water, which will comprise an increasing proportion of the outflow discharge. In such a situation, vertical heat exchange would be reduced and outflow temperatures could approach those predicted by the epilimnion model. Smith et al. (1982) observed consistent overflows in a small proglacial lake with low sediment input. Weirich (1986) found that overflows reached all the way to the outflow channel only when inflow suspended sediment concentration was at a minimum. While the glacier still exists, down-lake katabatic winds may encourage overflows to reach the outflow channel, thus displacing warm surface water and resulting in higher stream temperatures.

It is possible that the shift in lake stability that was observed on around 7 August was caused by the transition from snow- to glacier ice-melt.. While this period was not associated with lower inflow discharge, it may have coincided with the surpassing of a threshold of inflow sediment concentration due to the additional sediment contained in glacier discharge. The associated increase in inflow density may have induced underflows for the first time during the summer. A faster depletion of winter snow cover may cause this shift to occur earlier in the summer. While

lower outflow temperatures might persist initially as earlier inflows are comprised of sediment laden glacier ice-melt, diminished flows and a longer inflow channel may eventually extinguish this effect.

4.3.2 Altered proglacial stream temperatures

Keeping all other variables constant, reducing the stream discharge in Model 4b had the effect of reducing the amount of stream warming that occurred throughout the alpine reach. Figure 4.1 outlines the potential effects of reduced discharge based on the processes inferred from interpretation of the hybrid models. It can be seen that some processes may have a warming effect (e.g. reduced stream surface albedo, increased bed heat exchange), while others may have a cooling effect (e.g. reduced turbulent fluxes, reduced surface area). Note there are a

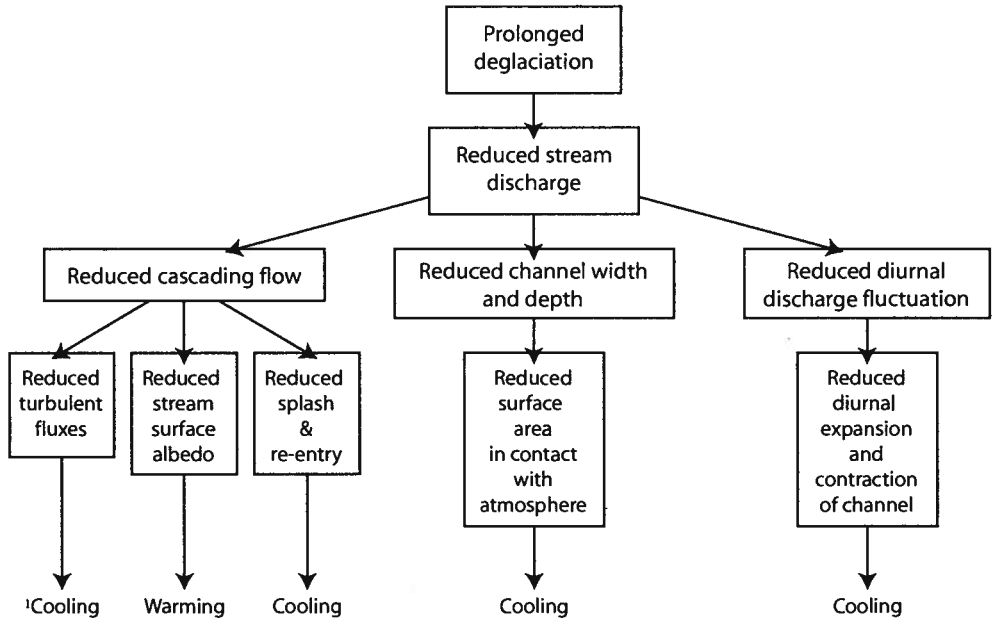

Figure 4.1: Inferred process responses to prolonged deglaciation from the hybrid heat budget modelling exercise

number of important processes that have not been investigated in this study and so have not been included in Figure 4.1. Examples include the effect of travel times on the magnitude of surface heat fluxes, the changing influence of lateral inputs from residual summer snowpack, and of course the variety of meteorological variables that will be altered with climate change.

Chapter 5

Conclusions

5.1 Summary of key findings

5.1.1 Place Lake

Place Lake had a consistent warming effect of 1-3°C (average 1.8°C) on inflowing water throughout the study period. Inflow temperatures were higher than expected and subject to significant heat input upstream of the inflow to Place Lake. The heat content of Place Lake was controlled mostly by (1) the heat flux associated with high volume inflows and outflows and (2) surface heating from absorbed shortwave radiation.

Modelling outflow temperatures cannot be achieved by simple physically based heat budget models. Outflow temperatures are not only a result of the lake heat content, but also cycles of mixing and stratification within the lake. Place Lake is neither well mixed nor consistently stratified in the late summer. The onset of glacier ice-melt may be linked to a shift in lake stability, and is a crucial indicator of the sensitivity of the current mixing regime. Unlike in most temperate lakes, mixing is dominated by inflow sediment load rather than convection currents induced by surface warming/cooling, or wind-induced turbulence. Water temperature is usually cited as the dominant control over density, but here it appears subordinate to the influence of the sediment content of large inflows. This finding is consistent with the work of Weirich (1986) who reported consistent isothermal conditions due to sediment-driven underflows in a similar high-energy proglacial lake.

Given that the most important assumption of DYRESM was that of minimal lateral mixing, it was encouraging to replicate water column temperatures at Place Lake with reasonable

precision, given the relatively high inflows and low residence time of through flowing water. Mixing in shallow, high-energy proglacial lakes appears to be controlled by a threshold of inflow density which is controlled by sediment content. At present, Place Lake appears to be in a state in which this threshold is periodically exceeded, thus producing complex patterns of mixing and stratification.

5.1.2 Alpine reach

A simple physically based heat budget model failed to reproduce observed stream warming at Place Creek. Hybrid physical-statistical modelling suggested that processes were misrepresented due to (1) steep terrain, which causes spatial variability in net radiation, (2) cascading, frothy flow, which results in a high stream surface albedo that varies with discharge, as well as and enhanced sensible and latent heat fluxes, and (3) highly variable late summer discharge, which prevents accurate estimation of stream width.

Alpine proglacial streams are particularly susceptible to warming due to (1) steep channel gradients which result in significant loss of potential energy and frictional heating over short distances, and (2) the intense solar insolation caused by lack of shade and high elevation. Consequences of glacier retreat might include a loss of cascading flow, reduced channel width and depth and reduced diurnal discharge fluctuations. While the modelling exercise indicated that reduced flows might lead to less downstream warming, it has been hypothesised that this effect would be the net result of a combination of different processes with contrasting effects, as outlined in Figure 4.1. Furthermore, the statistical model is strictly only valid for the range of discharges in the data used for model fitting (extrapolating this was an exploratory exercise). The relation between stream warming and discharge could be non-monotonic, whereby it is, for example, negative for low flows and then shifts to positive for higher flows.

Spatially distributed radiation modelling provided a straightforward alternative to extensive field measurements that would be required to account for the spatial variability in topographic

shading throughout the alpine reach, as well as the slope and aspect of the channel. An ideal application of the model would be to a Lagrangian heat budget model, in which the temperature of a parcel of water is estimated over both space and time. This requires, however, an accurate estimate of the velocity of the flow, which can be measured using salt dilution gauging.

5.2 Future research

While this study has generated new insights into the thermal behaviour of proglacial lakes and streams, it has also highlighted a number of key knowledge gaps, some of which could not be addressed in the current work due to lack of appropriate field measurements.

In terms of the thermal regime of proglacial lakes, a key finding is that Place Lake exhibited a diurnal cycle of mixing and stratification, which could be captured within DYRESM by changing the depth of inflow based on a threshold discharge. These points lead to the hypothesis that the split based on discharge accounts for diurnal variations in density associated with changes in suspended sediment concentrations. Unfortunately, suspended sediment concentrations in the inflow were not monitored in this study.

There is a need, therefore, for a detailed study of a single high-energy proglacial lake, focused on sediment-driven density currents. Essential measurements would include recording the bathymetry of the lake and spatially distributed sampling of suspended sediment and water temperature. This study would provide a direct comparison to the work of Weirich (1986) and thus strengthen the current knowledge of proglacial lake mixing. In addition, a heat budget analysis (similar to the one conducted here) should be carried out, so that the results are relevant in the context of proglacial alpine stream temperatures. Place Lake is a particularly good study site because of (1) the single inflow and outflow channel, and low residence time of through-flowing water, and (2) the fact that cycles of both mixing and stratification have been observed which increases the potential to understand the controls on both mixing and

stratification. Specific questions to be addressed in such studies include the following:

- Is inflow suspended sediment concentration correlated with outflow temperatures in shallow, high-energy proglacial lakes?
- To what extent does a threshold in inflow suspended sediment concentration govern the occurrence of underflows or overflows?
- Are density driven underflows the biggest driver of mixing?
- How does the bathymetry of the lake influence patterns of mixing and stratification?

In relation to the thermal regime of proglacial streams, this study demonstrated that simple models based on approaches developed for low-gradient streams are not applicable to steep alpine reaches. Future research should extend the heat budget analysis to include measurements of stream-surface albedo to provide a direct test of the parameterised relation with discharge and also velocity measurements to allow travel time to be explicitly modelled, e.g., using a Lagrangian model that tracks the temperature changes of parcels of water as they flow downstream. Ideally, the heat-budget analysis should be conducted in a reach for which reliable discharge measurements can be made at different locations along the reach, to allow estimation of lateral inflow (which was assumed negligible in this study due to the difficulty in measuring discharge in the lower portions of the reach).

Further work should address the parameterisation of the sensible and latent heat fluxes as a function of flow regime. It may be beneficial to conduct a laboratory flume study to allow as much control as possible over the radiative and conductive fluxes at the stream surface and bed. Another potentially important mode of heat transport is the transfer of heat from channel substrate (particularly boulders) to the water during rising flow. This process could be studied by embedding thermocouples into holes drilled into boulders at different locations and computing heat conduction via Fouriers law.

Extending beyond the alpine reach, there is a need for research on the processes controlling temperature of water reaching valley-bottom reaches, which are often important salmonid habitat. Given that travel times from the alpine to valley bottom sites may be several hours, a steady-state model will not be appropriate. Therefore, there is a need to consider not just the heat exchange processes in steep channels, but also the hydraulics and flow routing.

References

Beschta, R. L., Bilby, R. E., Brown, G. W., Holtby, L. B., and Hofstra, T. D. (1987). Stream temperature and aquatic habitat: fisheries and forestry interactions. In Salo, E. O. and Cundy, T. W., editors, *Streamside Management: Forestry and Fishery Interactions*, volume number 57, pages 191–232. Institute of Forest Resources, University of Washington.

Brown, G. W. (1969). Predicting temperatures of small streams. *Water Resources Research*, 5:68–75.

Brown, L. E., Hannah, D. M., and Milner, A. M. (2005). Spatial and temporal water column and streambed temperature dynamics within an alpine catchment: implications for benthic communities. *Hydrological Processes*, 19(8):1585–1610.

Brown, L. E., Hannah, D. M., and Milner, A. M. (2006). Hydroclimatological influences on water column and streambed thermal dynamics in an alpine river system. *Journal of Hydrology*, 325(1-4):1–20.

Cadbury, S. L., Hannah, D. M., Milner, A. M., Pearson, C. P., and Brown, L. E. (2008). Stream temperature dynamics within a New Zealand glacierized river basin. *River Research and Applications*, 24:68–89.

Chapra, S. C. (1997). *Surface Water-Quality Modeling.* McGraw-Hill New York.

Chikita, K. A., Smith, N. D., Yonemitsu, N., and Perez-Arlucea, M. (1996). Dynamics of sediment-laden underflows passing over a subaqueous sill: glacier-fed Peyto Lake, Alberta, Canada. *Sedimentology*, 43(5):865–875.

Collins, D. N. (1987). Climatic Fluctuations and Runoff from Glacierised Alpine Basins. *IAHS-AISH publication*, (168):77–89.

Erbs, D. G., Klein, S. A., and Duffie, J. A. (1982). Estimation of the diffuse radiation fraction for hourly, daily and monthly-average global radiation. *Solar Energy*, 28(4):293–302.

Evans, E. C., McGregor, G. R., and Petts, G. E. (1998). River energy budgets with special reference to river bed processes. *Hydrological Processes*, 12(4):575–595.

Fleming, S. W. (2005). Comparative analysis of glacial and nival streamflow regimes with implications for lotic habitat quantity and fish species richness. *River Research and Applications*, 21(4):363–379.

Frempong, E. (1983). Diel aspects of the thermal structure and energy budget of a small English lake. *Freshwater Biology*, 13(1):89–102.

Gibson, C. E. and Stewart, D. A. (1973). The annual temperature cycle of Lough Neagh. *Limnology and Oceanography*, 18(5):791–793.

Gilbert, R. and Butler, R. D. (2004). The physical limnology and sedimentology of Meziadin Lake, northern British Columbia, Canada. *Arctic, Antarctic, and Alpine Research*, 36(1):33–41.

Gilbert, R. and Shaw, J. (1981). Sedimentation in proglacial Sunwapta Lake, Alberta. *Canadian Journal of Earth Sciences*, 18(1):81–93.

Gu, R., Montgomery, S., and Austin, T. A. (1998). Quantifying the effects of stream discharge on summer river temperature. *Hydrological Sciences Journal*, 43:885–904.

Guenther, S. M. (2007). Impacts of partial-retention harvesting with no buffer on the thermal regime of a headwater stream and its riparian zone. Unpublished MSc thesis, The University of British Columbia, Vancouver.

Gustavson, T. C. (1975). Sedimentation and physical limnology in proglacial Malaspina Lake, southeastern Alaska. *Glaciofluvial and Glaciolacustrine Sedimentation: Society of Economic Paleontologists and Mineralogists, Special Publication*, 23:249–263.

Hannah, D. M., Brown, L. E., Milner, A. M., Gurnell, A. M., McGregor, G. R., Petts, G. E., Smith, B. P. G., and Snook, D. L. (2007). Integrating climate-hydrology-ecology for alpine river systems. *Aquatic Conservation: Marine and Freshwater Ecosystems*, 17:636–656.

Hannah, D. M., Malcolm, I. A., Soulsby, C., and Youngson, A. F. (2008). A comparison of forest and moorland stream microclimate, heat exchanges and thermal dynamics. *Hydrological Processes*, 22:919–940.

Harris, P. W. V. (1976). The seasonal temperature-salinity structure of a glacial lake: Jökulsarlon, south-east Iceland. *Geografiska Annaler*, 58:329–336.

Hock, R., Jansson, P., and Braun, L. (2005). Modelling the response of mountain glacier discharge to climate warming. *Global Change and Mountain Regions (A State of Knowledge Overview)*, pages 243–252.

Hockey, J. B., Owens, I. F., and Tapper, N. J. (1982). Empirical and theoretical models to isolate the effect of discharge on summer water temperatures in the Hurunui River. *Journal of Hydrology (NZ)*, 21(1):1–12.

Imerito, A. (2007). *Dynamic Reservoir Simulation Model DYRESM v4 Science Manual.* Centre for Water Research, University of Western Australia.

Iqbal, M. (1983). *An Introduction to Solar Radiation.* Academic Press, Toronto; New York.

Klein, R. D. (1979). Urbanization and stream quality impairment. *Water Resources Bulletin*, 15(4):948–963.

Malard, F., Mangin, A., Uehlinger, U., and Ward, J. V. (2001). Thermal heterogeneity in the hyporheic zone of a glacial floodplain. *Canadian Journal of Fisheries and Aquatic Sciences*, 58(7):1319–1335.

Malcolm, I. A., Soulsby, C., Youngson, A. F., Hannah, D. M., McLaren, I., and Thorne, A. (2004). Hydrological influences on hyporheic water quality: implications for salmon egg survival. *Hydrological Processes*, 18(9):1543–1560.

Mathews, W. H. (1956). Physical limnology and sedimentation in a glacial lake [British Columbia]. *Bulletin of the Geological Society of America*, 67(5):537–552.

Milner, A. M., Brittain, J. E., Castella, E., and Petts, G. E. (2001). Trends of macroinvertebrate community structure in glacier-fed rivers in relation to environmental conditions: a synthesis. *Freshwater Biology*, 46(12):1833–1847.

Mohseni, O., Stefan, H. G., and Eaton, J. G. (2003). Global warming and wotential changes in fish habitat in US streams. *Climatic Change*, 59(3):389–409.

Moore, R. D. (2005a). Slug Injection Using Salt in Solution. *Streamline Watershed Management Bulletin*, 8 (2):1–6.

Moore, R. D. (2005b). Stream Temperatures in British Columbia: Regional Patterns and Prediction. *A progress report submitted to the Ministry of Water, Land and Air Protection.*

Moore, R. D. (2006). Stream temperature tatterns in British Columbia, Canada, based on routine spot measurements. *Canadian Water Resources Journal*, 31:41–56.

Moore, R. D. and Demuth, M. N. (2001). Mass balance and streamflow variability at Place Glacier, Canada, in relation to recent climate fluctuations. *Hydrological Processes*, 15(18):3473–3486.

Moore, R. D., Spittlehouse, D. L., and Story, A. (2005a). Riparian microclimate and stream temperature response to forest harvesting: a review. *Journal of the American Water Resources Association*, 41(4):813–834.

Moore, R. D., Sutherland, P., Gomi, T., and Dhakal, A. (2005b). Thermal regime of a headwater stream within a clear-cut, coastal British Columbia, Canada. *Hydrological Processes*, 19(13):2591–2608.

Morrill, J. C., Bales, R. C., Asce, M., and Conklin, M. H. (2005). Estimating stream temperature from air temperature: implications for future water quality. *Journal of Environmental Engineering*, 131(1):139–46.

Moshfeghi, H., Etemad-Shahidi, A., and Imberger, J. (2005). Modelling of bubble plume destratification using DYRESM. *Aqua- Journal of Water Supply: Research and Technology*, 54(1):37–46.

Oke, T. R. (1987). *Boundary Layer Climates*. Routledge, London, GB.

Potts, D. J. (2004). The heat budget of Quesnel Lake, British Columbia. Unpublished MSc thesis, The University of British Columbia, Vancouver.

Quinn, J. M., Cooper, A. B., Davies-Colley, R. J., Rutherford, J. C., and Williamson, R. B. (1997). Land use effects on habitat, water quality, periphyton, and benthic invertebrates in

Waikato, New Zealand, hill-country streams. *New Zealand Journal of Marine and Freshwater Research*, 31(5):579–597.

Richards, G. and Moore, R. D. (2003). Suspended sediment dynamics in a steep, glacier-fed mountain stream, Place Creek, Canada. *Hydrological Processes*, 17(9):1733–1753.

Robinson, C. T. and Matthaei, S. (2007). Hydrological heterogeneity of an alpine stream–lake network in Switzerland. *Hydrological Processes*, 21:3146–3154.

Rutherford, J. C., Blackett, S., Blackett, C., Saito, L., and Davies-Colley, R. J. (1997). Predicting the effects of shade on water temperature in small streams. *New Zealand Journal of Marine and Freshwater Research*, 31(5):707–721.

Schertzer, W. M. (1978). Energy budget and monthly evaporation estimates for Lake Superior, 1973. *Journal of Great Lakes Research*, 4:320–330.

Smith, N. D., Venol, M. A., and Kennedy, S. K. (1982). Comparison of sedimentation regimes in four glacier-fed lakes of western Alberta. *Research in Glacial, Glacio-Fluvial and Glacio-Lacustrine Systems. Proceedings of the 6 th Guelph Symposium on Geomorphology, 1980.*, pages 203–238.

Stahl, K. and Moore, R. D. (2006). Influence of watershed glacier coverage on summer streamflow in British Columbia, Canada. *Water Resources Research*, 42(6):6201.

Stull, R. B. (2000). *Meteorology for Scientists and Engineers.* Brooks/Cole Pacific Grove, CA.

Sturm, M. and Matter, A. (1978). Turbidities and varves in Lake Brienz (Switzerland): Deposition of elastic detritus by density currents. *Publications of the International Association of Sedimentology*, 2:147–168.

Uehlinger, U., Malard, F., and Ward, J. V. (2003). Thermal patterns in the surface waters of a glacial river corridor(Val Roseg, Switzerland). *Freshwater Biology*, 48(2):284–300.

Warren, C. R. and Kirkbride, M. P. (1998). Temperature and bathymetry of ice-contact lakes in Mount Cook National Park, New Zealand. *New Zealand Journal of Geology and Geophysics*, 41(2):133–143.

Webb, B. W., Clack, P. D., and Walling, D. E. (2003). Water-air temperature relationships in a Devon river system and the role of flow. *Hydrological Processes*, 17(15):3069–3084.

Webb, B. W. and Zhang, Y. (1997). Spatial and seasonal variability in the components of the river heat budget. *Hydrological Processes*, 11(1):79–101.

Webb, B. W. and Zhang, Y. (1999). Water temperatures and heat budgets in Dorset chalk water courses. *Hydrological Processes*, 13(3):309–321.

Weirich, F. (1986). The record of density-induced underflows in a glacial lake. *Sedimentology*, 33(2):261–277.

Wetzel, R. G. (1975). *Limnology*. W.B. Saunders Company, Philadelphia.

Willmott, C. J. (1982). Some Comments on the Evaluation of Model Performance. *Bulletin of the American Meteorological Society*, 63(11):1309–1313.